administration is also applicable to deliver siRNA- and shRNA-expressing pDNA to tumor cells in the liver.[18] Therefore, the hydrodynamics-based procedure can be an effective method to suppress the growth of tumor cells that are metastasized to the liver. Because the hydrodynamic administration can induce RNAi in both tumor cells in the liver and normal liver cells, suppressing the increased expression of a gene that aggravates the metastatic tumor growth in both tumor and liver cells can be an effective approach in treating hepatic metastasis. To this end, we selected HIF-1α as such a target gene in the present study. We applied the hydrodynamic injection method to administer shRNA-expressing pDNA targeting HIF-1α (pshHIF-1α) and found that the suppression of HIF-1α expression in the liver can suppress the growth of metastasizing tumor cells in that organ. Moreover, selective suppression of HIF-1α expression only in normal liver cells was found to be also effective in inhibiting metastatic tumor growth, indicating that HIF-1α expression in normal cells assisted the tumor progression.

Results

Reduction in protein expression of HIF-1α by shRNA-expressing pDNA

As previously reported by several groups, an enzyme-linked immunosorbent assay (ELISA) analysis showed that addition of $CoCl_2$ increased the amount of HIF-1α proteins in Colon26 and B16-BL6 cells (Figure 1a). Similar results were obtained when HIF-1α protein levels in Colon26 cells were evaluated by western blot analysis (Figure 1b). Transfection of pshHIF-1α reduced the amount of HIF-1α protein, whereas transfection of control pDNA or pshGFP (green fluorescent protein) hardly affected the level of HIF-1α expression.

Using immunofluorescent staining with HIF-1α-specific antibody, localization of HIF-1α protein in the cells was visualized. While a weak signal of HIF-1α was observed in cytoplasm when cells were incubated without $CoCl_2$, incubation of Colon26 cells with $CoCl_2$ resulted in nuclear accumulation of HIF-1α, which was detected as yellow signals as a result of overlap between the green fluorescence derived from HIF-1α and the red fluorescence derived from nuclear staining (Figure 1c). Transfection of pshHIF-1α reduced the number of cells that show HIF-1α accumulation in their nucleus.

Inhibition of HIF-1 transcriptional activity by pshHIF-1α

To investigate whether pshHIF-1α is effective in suppressing the transcription activity of HIF-1, cells were transfected with a pDNA encoding luciferase gene under the control of hypoxia response element (HRE). In Colon26 cells, HRE-dependent luciferase expression from the reporter pDNA co-transfected with control pDNA or pshGFP was moderately increased by the addition of $CoCl_2$. However, in B16-BL6 cells, HRE-dependent luciferase expression was increased by the addition of $CoCl_2$ compared with Colon26 cells (Figures 2a and b). HRE-dependent luciferase expression in the presence of $CoCl_2$ was almost completely inhibited to about the expression level observed in the absence of $CoCl_2$ by transfection of pshHIF-1α.

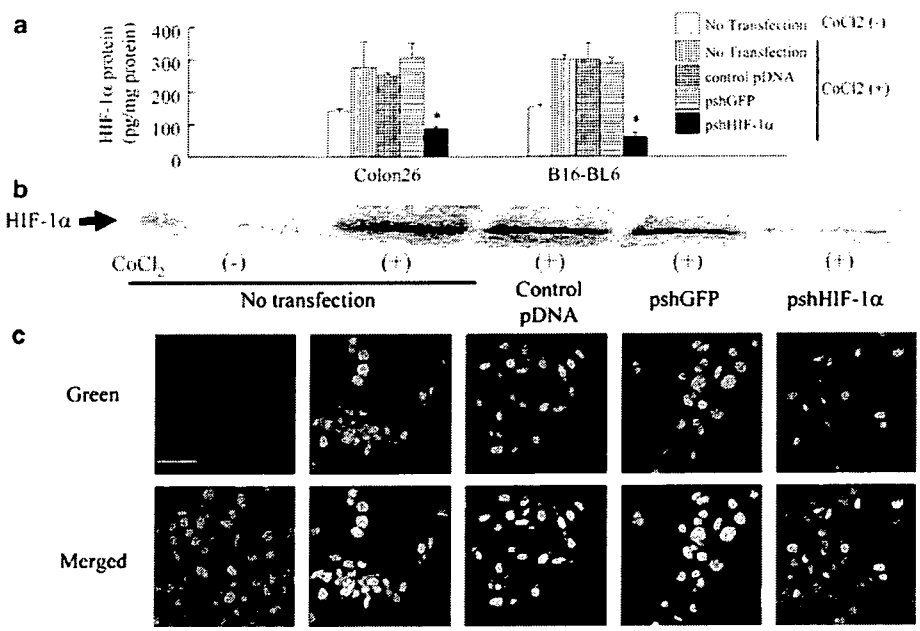

Figure 1 Hypoxia-inducible factor-1α (HIF-1α) protein expression level in tumor cells following transfection of short hairpin (shRNA)-expressing plasmid DNA (pDNA). Cells were transfected with control pDNA, pshGFP (green fluorescent protein) or pDNA expressing shRNA targeting HIF-1α (pshHIF-1α). At 4 h after transfection, cells were washed with phosphate-buffered saline (PBS) and then cultured with growth medium supplemented with or without 100 μM $CoCl_2$ for an additional 20 h. (**a**) Enzyme-linked immunosorbent assay (ELISA) analysis of HIF-1α protein from cell lysates of Colon26 or B16-BL6 cells. The results are expressed as the mean ± s.d. of three samples. $^*P < 0.05$ for Student's *t*-test versus the control group. (**b**) Western blotting analysis of HIF-1α for cell lysates of Colon26 cells. (**c**) Immunofluorescent staining of HIF-1α in transfected Colon26 cells. HIF-1α protein expression was detected as a green color, and the cell nucleus was stained with propidium iodide (red). Yellow signals indicate that HIF-1α localizes in the cell nucleus. Scale bar = 50 μm.

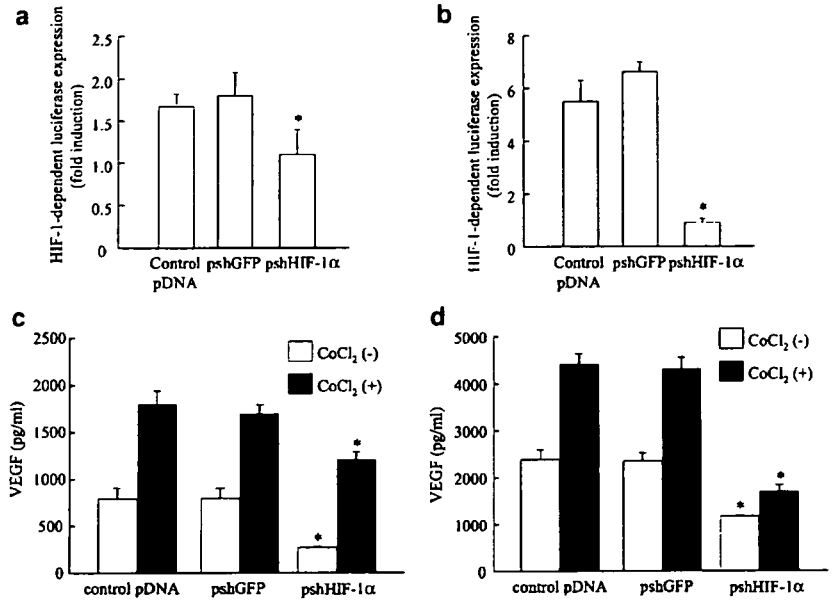

Figure 2 Suppression of hypoxia-inducible factor-1 (HIF-1)-dependent gene expression by transfection of plasmid DNA (pDNA) expressing shRNA targeting HIF-1α (pshHIF-1α). (**a**, **b**) Suppression of HIF-1-dependent reporter gene expression by pshHIF-1α. pLuc-HRE and phRL-TK were co-transfected with control pDNA, pshGFP (green fluorescent protein) or pshHIF-1α to Colon26 (**a**) or B16-BL6 (**b**) cells. At 4 h after transfection, cells were washed with phosphate-buffered saline (PBS) and cultured in medium with or without 100 μM $CoCl_2$ for an additional 20 h. Luciferase activities were measured 24 h after transfection. The results are expressed as the mean ± s.d. of three samples. (**c**, **d**) Reduction in HIF-1-dependent vascular endothelial growth factor (VEGF) production by pshHIF-1α. Colon26 (**c**) or B16-BL6 (**d**) cells were transfected with control pDNA, pshGFP or pshHIF-1α. At 4 h after transfection, cells were washed with PBS and cultured in medium with or without 100 μM $CoCl_2$ for an additional 44 h. The amount of VEGF protein in the cultured medium was measured 48 h after transfection using enzyme-linked immunosorbent assay (ELISA). The results are expressed as the mean ± s.d. of three samples. $^*P<0.05$ for Student's *t*-test versus the control group.

To further estimate the effect of pshHIF-1α transfection on the expression of VEGF, an endogenous gene product of HIF-1 transcription activity, culture media of tumor cells were collected 48 h after the transfection. The VEGF concentration in the supernatant was measured by ELISA (Figures 2c and d). In both cell lines, about a two-fold increase was detected in the VEGF from $CoCl_2$-treated cells compared with that from untreated cells. In Colon26 cells, transfection of pshHIF-1α reduced VEGF secretion to about one-third or two-thirds of the control values without or with $CoCl_2$, respectively. In B16-BL6 cells, transfection of pshHIF-1α reduced VEGF secretion to about half or one-third of the control values without or with $CoCl_2$, respectively.

Increase in HIF-1α expression in the liver by tumor inoculation via the portal vein

Mice were inoculated with tumor cells into the portal vein, and received an intravenous injection of each pDNA 5 days after tumor inoculation. Then, immunofluorescent staining of liver sections was performed to detect HIF-1α protein expression 7 days after tumor inoculation. Representative images are shown in Figures 3a–g. No significant signal of HIF-1α was observed in the liver sections of naïve mice, sham-operated mice and those receiving control pDNA (Figures 3a–c). In contrast, a strong HIF-1α signal was observed in the liver sections of tumor-bearing mice (Figure 3d). In these pictures, increased HIF-1α expression was mainly observed in hepatic cells. Administration of control pDNA or pshGFP had little effect on HIF-1α expression induced by the inoculation of tumor cells (Figures 3e and f). Moreover, hydrodynamic administration of pshHIF-1α reduced the signal intensity derived from HIF-1α protein compared with other tumor-bearing groups (Figure 3g). By quantitatively analyzing relative areas of the HIF-1α expression (green signal) to the total area in the images, the percentage inhibition by pshHIF-1α was calculated to be about 20–30% of the other tumor-bearing groups. In addition, the administration of pshHIF-1α significantly ($P<0.05$) reduced the mRNA expression of HIF-1α in tumor-bearing liver, from 0.0059 ± 0.0011 copies relative to GAPDH mRNA (the control pDNA-treated group) to 0.0021 ± 0.0005.

Suppression of HIF-1α expression in liver by the pre-administration of pshHIF-1α

As it had been demonstrated that tumor inoculation via the portal vein induced HIF-1α accumulation in liver cells, we investigated whether the delivery of pshHIF-1α only to liver cells, not to tumor cells, affects tumor growth in the liver. To this end, tumor cells were inoculated 3 days after the hydrodynamic administration of pDNAs. Immunofluorescent staining for HIF-1α was performed at 2 days after tumor inoculation to investigate the HIF-1α expression level at that time (Figures 3h–l). Similar to the results of the sample prepared at 7 days after tumor inoculation, a strong signal derived from HIF-1α protein was detected in the liver sections prepared at 2 days after tumor inoculation (Figure 3i).

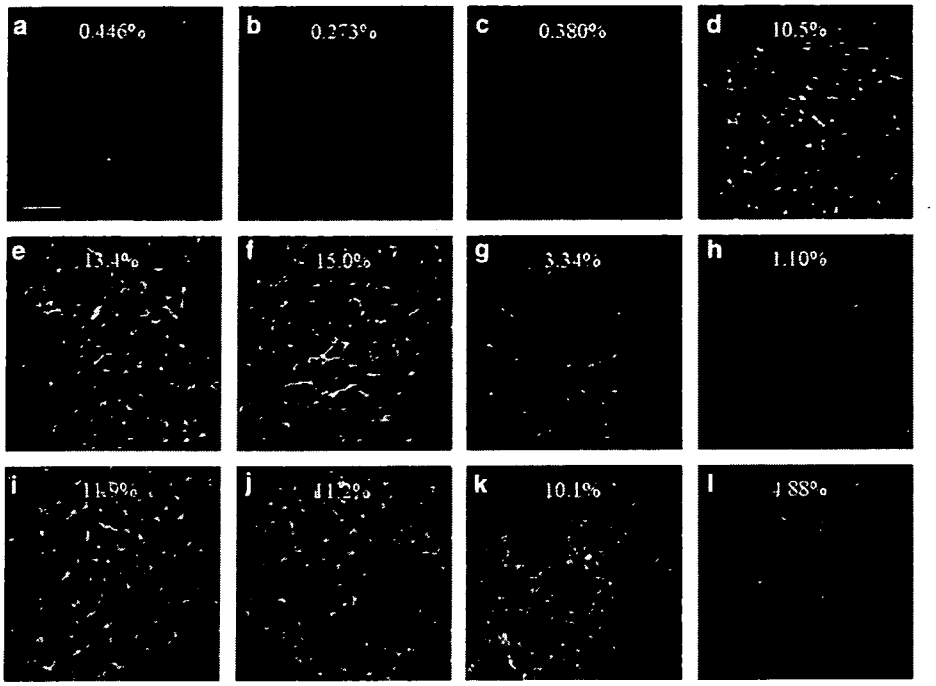

Figure 3 Hypoxia-inducible factor-1α (HIF-1α) expression in the liver of tumor-bearing mice. Some mice were untreated (**a**) or received plasmid DNA (pDNA) only (**b**). The sham operation group (**c**) received only an intraportal injection of Hank's balanced salt solution (HBSS) solution without tumor cells. At 5 days after tumor inoculation via the portal vein, mice were untreated (**d**) or received an intravenous injection of control pDNA (**e**), pshGFP (green fluorescent protein) (**f**) or pDNA expressing shRNA targeting HIF-1α (pshHIF-1α) (**g**). At 2 days after pDNA administration, liver samples were collected and subjected to immunostaining for HIF-1α. The sham operation group received only an intraportal injection of HBSS solution without tumor cells (**h**). At 3 days before tumor inoculation via the portal vein, mice were untreated (**i**) or received an intravenous injection of control pDNA (**j**), pshGFP (**k**) or pshHIF-1α (**l**). At 2 days after tumor inoculation, liver samples were collected and subjected to immunostaining for HIF-1α. Scale bar = 50 μm. Numbers in the images represent the relative area of HIF-1α expression (green signal) to the total area. See online version for color figure.

pshHIF-1α administrated before tumor inoculation suppressed the induction of HIF-1α expression by tumor inoculation (Figure 3l). Administration of irrelevant pDNAs did not change the expression level of HIF-1α in the liver (Figures 3j and k). Quantification of the relative areas of the HIF-1α expression (green signal) to the total area in the images indicated that pre-administration of pshHIF-1α reduced HIF-1α expression to about 50% of the other tumor-inoculated groups.

Location of HIF-1α expression in the tumor-inoculated liver relative to tumor cells

To visualize Colon26 cells in the liver, Colon26 cells transfected with pDsRed2-N1 were inoculated into the portal vein of mice. Immunofluorescent staining for HIF-1α was performed at 2 days after tumor inoculation to investigate the location of HIF-1α expression relative to tumor cells (Figures 4a–d). DsRed-labeled Colon26 cells were found in some liver sections, and almost all of these cells were surrounded by liver cells expressing an increased level of HIF-1α (Figures 4a and b). Some liver cells not close to Colon26 cells also showed a high HIF-1α expression (Figure 4c), but most other liver cells hardly expressed the protein (Figure 4d). These results suggest that tumor cells entrapped in the hepatic capillaries is closely associated with the increased expression of HIF-1α in the surrounding liver cells.

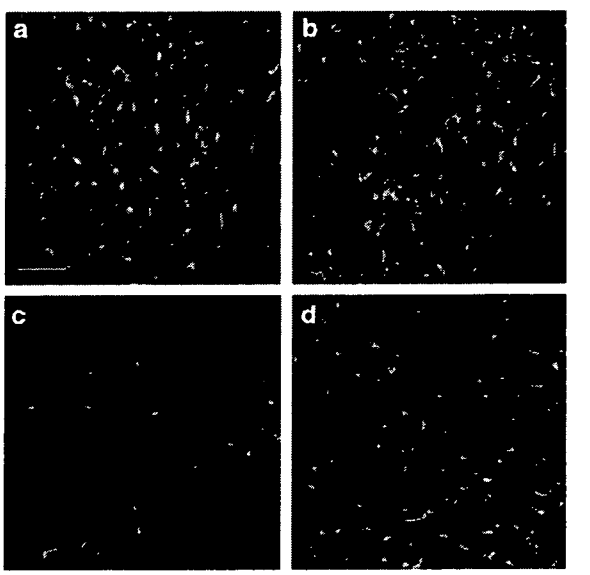

Figure 4 Location of hypoxia-inducible factor-1α (HIF-1α) expression in the tumor-bearing liver relative to tumor cells. At 2 days after tumor inoculation, liver samples were collected and subjected to immunostaining for HIF-1α. Red signals represent Colon26 cells expressing DsRed, and green signals represent HIF-1α protein. Representative images of liver sections positive (**a**, **b**) or negative (**c**, **d**) for DsRed-labeled Colon26 cells are indicated. Scale bar = 50 μm.

Induction of MMP-2 and -9 expression in the liver by tumor inoculation via the portal vein

To evaluate the effect of tumor inoculation via the portal vein on the MMP expression in the liver, the amount of MMP in liver homogenate was measured by gelatin zymography 8 days after tumor inoculation (Figure 5a). As we have reported previously, MMP-2 and -9 activities in the homogenate of tumor-inoculated liver was higher than that of the untreated group. A hydrodynamic delivery of control pDNA or pshGFP 5 days after tumor inoculation had little or no effect on both types of MMP activity. No significant increase in the MMP activity was detected in the liver homogenate of sham-operated mice or mice that received only pDNA. Intravenous injection of pshHIF-1α by the hydrodynamics-based procedure 5 days after tumor inoculation clearly reduced the MMP-9 gelatinolytic activity in the liver of tumor-bearing mice compared with the other tumor-inoculated group. Less, but detectable, reduction was also observed in the MMP-2 activity.

To assess the effect of HIF-1α expression in normal cells on MMP production, pshHIF-1α was administered 3 days before tumor inoculation. Gelatin zymography was performed at 3 days after tumor inoculation (Figure 5b). At this time point, the sham operation group showed slightly increased MMP-9 activity compared with naïve mice. Although the increase in MMP-9 expression level in the liver at this time was smaller than that detected at 8 days after tumor inoculation, the homogenate of tumor-bearing liver showed a higher MMP-9 activity than the other tumor-free groups. Pretreatment of pshHIF-1α reduced MMP-9 induction by tumor inoculation, while preinjection of control pDNA and

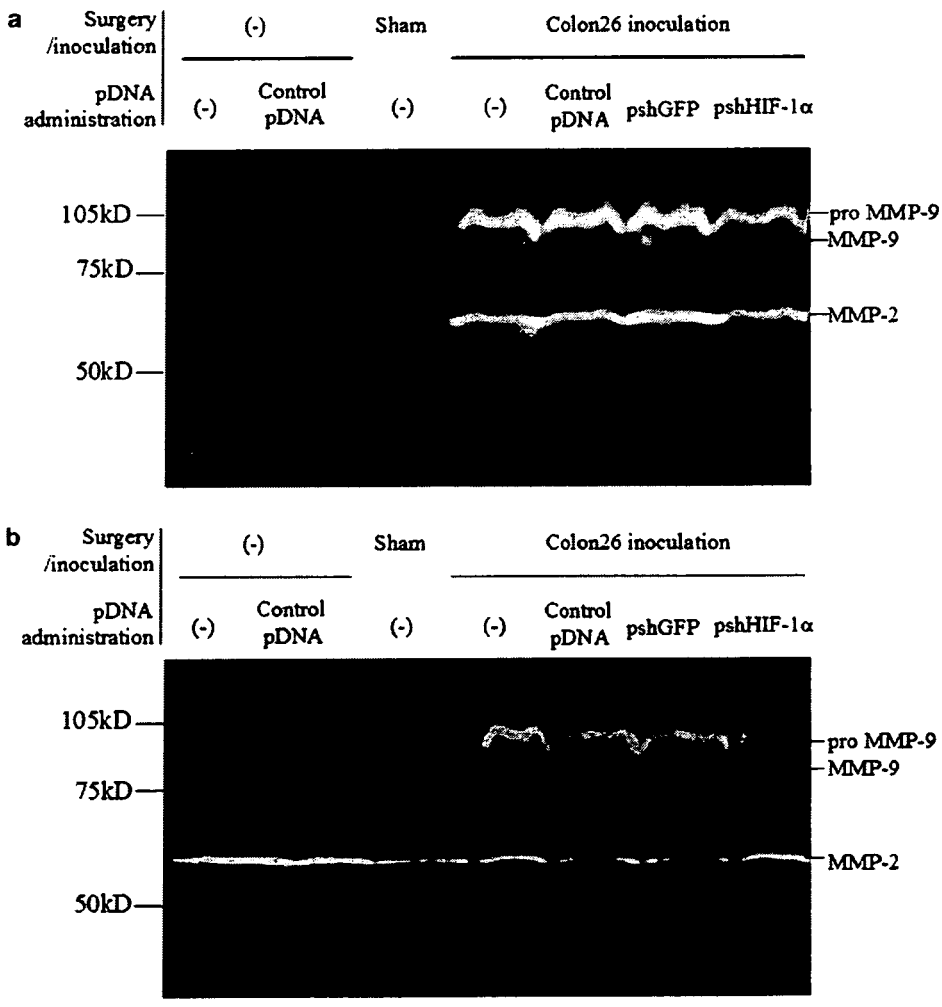

Figure 5 Gelatin zymography performed on liver samples. (**a**) At 5 days after tumor inoculation via the portal vein, mice received an intravenous injection of control plasmid DNA (pDNA), pshGFP (green fluorescent protein) or pDNA expressing shRNA targeting HIF-1α (pshHIF-1α). The sham operation group received only an intraportal injection of Hank's balanced salt solution (HBSS) solution without tumor cells. At 3 days after pDNA administration, liver samples were collected and subjected to gelatin gel zymography. Four mice of each group were used to analyze the matrix metalloproteinase (MMP) expression, and typical results are shown. (**b**) At 3 days before tumor inoculation via the portal vein, mice received an intravenous injection of control pDNA, pshGFP or pshHIF-1α. The sham operation group received only an intraportal injection of HBSS solution without tumor cells. At 3 days after tumor inoculation, liver samples were collected and subjected to gelatin gel zymography. Four mice of each group were used to analyze the MMP expression, and typical results are shown.

pshGFP had little effect on MMP-9 induction in the liver following tumor inoculation. We did not observe any obvious difference in MMP-2 production between tumor-free and tumor-bearing groups.

Suppression of metastatic tumor growth in the liver by pshHIF-1α

Figure 6a shows the tumor cell number in the liver, which was evaluated by measuring tumor-derived luciferase activities at 1 week after pDNA administration (Figure 6a). Mice were inoculated with Colon26 cells into the portal vein, and each pDNA was injected into the tail vein with 5-day interval. Control pDNA or pshGFP hardly reduced the number of tumor cells, while pshHIF-1α significantly ($P<0.05$) reduced the number to about, on average, 1–2% of the other groups. Many large tumor nodules were found in the frozen liver sections of mice receiving control pDNA (Figure 6c). In a quite contrast, much small and few tumor nodules were detected in the sections of mice receiving pshHIF-1α (Figure 6d). These hematoxylin and eosin-stained sections strongly support the quantitative results of metastatic tumor growth estimated using the luciferase activity of Colon26/Luc cells (Figure 6a).

Next, we investigated the effect of preadministration of pshHIF-1α on the growth of tumor cells in the liver by estimating the tumor cell number 12 days after tumor inoculation (Figure 6b). As a result, pshHIF-1α preadministration 3 days before tumor inoculation significantly reduced the number of tumor cells in the liver 12 days after tumor inoculation compared with the groups that were untreated or given pDNA. On average,

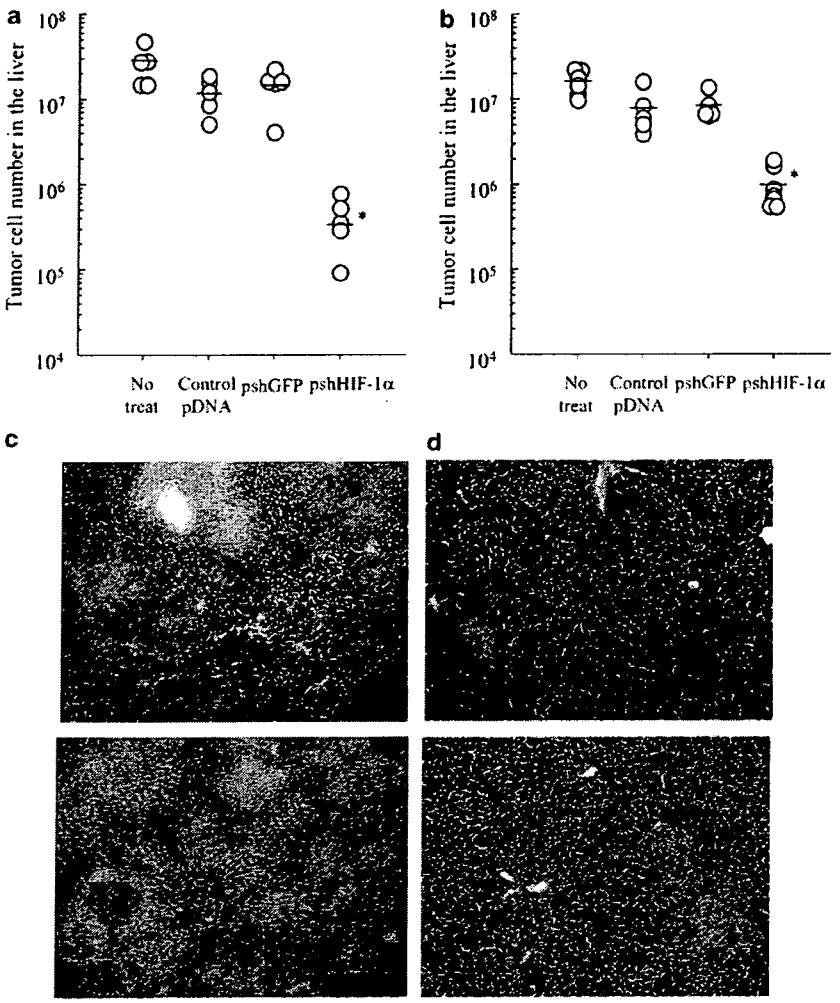

Figure 6 Number of Colon26/Luc cells in mouse liver 12 days after tumor inoculation. (**a**) At 5 days after tumor inoculation via the portal vein, mice received an intravenous injection of control plasmid DNA (pDNA), pshGFP (green fluorescent protein) or pDNA expressing shRNA targeting HIF-1α (pshHIF-1α). At 7 days after pDNA administration, liver samples were collected and the number of tumor cells was evaluated by measuring luciferase activities derived from Colon26/Luc cells. Open circles (○) indicate the tumor cell number in the liver of individual mice. Bars indicate the average tumor cell number of each group ($n=5$). *$P<0.05$ for Student's *t*-test versus untreated group. (**b**) At 3 days before tumor inoculation via the portal vein, mice received an intravenous injection of control pDNA, pshGFP or pshHIF-1α. At 12 days after tumor inoculation, liver samples were collected and the number of tumor cells was evaluated by measuring luciferase activities derived from Colon26/Luc cells. Open circles (○) indicate the tumor cell number in the liver of individual mice. Bars indicate the average tumor cell number of each group of at least five mice. *$P<0.05$ for Student's *t*-test versus untreated group. (**c**, **d**) Hematoxylin and eosin-stained liver sections of tumor-bearing mice receiving (**c**) control pDNA or (**d**) pshHIF-1α at 7 days after tumor inoculation. Scale bar = 200 μm. See online version for color figure.

preadministration of pshHIF-1α reduced the number of tumor cells to about 10% of other groups. The degree of reduction in the number of tumor cells by pshHIF-1α administered before tumor inoculation was about 5- to 10-fold less than that of pshHIF-1α administered after tumor inoculation.

Discussion

HIF-1α expression and subsequent HIF-1 activation in cancer cells play important roles in cancer progression by controlling the gene expression related to cancer cell proliferation, apoptosis and metastasis.[9] In the present study, we demonstrated that HIF-1α expression in normal hepatic cells is also increased by tumor cells entering the liver via the portal vein and that such HIF-1α expression aggravates tumor growth. Our results indicate the possibility of a novel therapeutic strategy for inhibiting metastatic tumor growth by silencing the HIF-1α expression in both normal and tumor cells.

Suppression of nuclear accumulation of HIF-1α by pshHIF-1α (Figure 1) was followed by inhibition of HIF-1-dependent transcription activities (Figure 2). In the experiment using pLuc-HRE, pshHIF-1α suppressed the transcription activity to almost the basal level in both Colon26 and B16-BL6 cells. Such an efficient inhibitory effect on luciferase expression might be because pLuc-HRE was co-transfected with pshHIF-1α, by which both pDNAs were delivered to the same cells. On the other hand, the suppressive effect of pshHIF-1α on VEGF production from B16-BL6 cells was much greater than that from Colon26 cells. Two factors may explain the difference in the efficiency of the inhibitory effect on VEGF production between B16-BL6 cells and Colon26 cells. One is the transfection efficiency of the pshHIF-1α. By using pDNA expressing enhanced green fluorescent protein (EGFP), we found that the transfection efficiency to B16-BL6 and Colon26 cells was about 80–90 and 70–80%, respectively, at 24 h after transfection (Y Takahashi *et al.*, unpublished data). Therefore, the difference in transfection efficiency between B16-BL6 and Colon26 cells may be one reason for the difference in suppressive effect on VEGF production by pshHIF-1α. The other reason for the difference in suppression in the two cell lines could be the contribution of HIF-1-dependent VEGF production to the total VEGF production. Other hypoxia-inducible transcriptional factors, such as HIF-2, are also known to be activated by $CoCl_2$ and increased HIF-2 expression might result in VEGF expression.[19]

When tumor cells were inoculated via portal vein, HIF-1α protein expression was increased in tumor-bearing liver (Figure 3). Inoculation of DsRed-labeled Colon26 cells clearly demonstrated that liver cells close to the tumor cells expressed HIF-1α at a high level (Figure 4). Oxygen concentration-dependent and -independent pathways might be considered as the mechanism for such an increase in HIF-1α expression. When tumor cells are inoculated via the portal vein, tumor cells are first arrested in small vessels, followed by extravasation, invasion of tissues and proliferation of tumor cells.[3] Therefore, blood flows would be, at least transiently, hindered by tumor cells, which could result in a reduction in the oxygen supply. In addition to hypoxia, other processes such as growth factor stimulation and cytokine stimulation are reported to increase HIF-1α expression and activate HIF-1-dependent transcription.[9,20] When tumor cells metastasize to the liver, expression of these secretary proteins might be induced and result in increased HIF-1α expression.

To distinguish the role of HIF-1α expressed in tumor cells from that in normal liver cells, pshHIF-1α was administered 3 days before tumor inoculation. As pDNA injected into the systemic circulation is very quickly degraded by nucleases and cleared by Kupffer and sinusoidal endothelial cells,[21] pDNA injected would have hardly any effects on the expression level of HIF-1α in Colon26/Luc cells. On the other hand, when pshHIF-1α was administered after tumor inoculation, pshHIF-1α might be delivered to both tumor and liver cells.[18] Therefore, pshHIF-1α administered before tumor inoculation might have been delivered only to normal cells in the liver, while pshHIF-1α administered after tumor inoculation might have been delivered to both tumor and normal cells in the liver.

In a previous study, we reported that Colon26 cell inoculation via the portal vein increased MMP-9 expression in the liver.[22] Elezkurtaj *et al.*[23] demonstrated that intrasplenic inoculation of CT-26 colon carcinoma cells, which form experimental liver metastases, increased MMP-2 and -9 expressions in liver tissue. In agreement with these results, we have found that MMP-9 is generated mainly from host cells, not the inoculated tumor cells (Y Takahashi *et al.*, unpublished data). There are some published papers reporting that MMP-9 expression is directly or indirectly regulated by HIF-1.[24–26] Therefore, we hypothesized that increased HIF-1 transcription activity in normal cells in the liver contributes to MMP-9 production induced by tumor cell inoculation. Intravenous administration of pshHIF-1α was effective in reducing the expression of MMP-9 after tumor inoculation, which indicates that HIF-1 expression in tumor cells and normal cells in the liver might play an important role in MMP-9 production. Moreover, administration of pshHIF-1α before tumor inoculation was found to be also effective in reducing the amount of MMP-9 in the liver. This result reinforces the hypothesis that normal cells in the liver, not tumor cells, are the major producer of MMP-9 and that MMP-9 expression is regulated by HIF-1. Although its role in metastatic tumor cell growth is still unclear, increased MMP expression is frequently accompanied by tumor metastasis and suppression of MMP expression could be used as a growth inhibitory treatment to prevent tumor metastasis.[23,27,28]

When pshHIF-1α was administered to tumor-bearing mice by the hydrodynamics-based procedure, a significant reduction in the number of tumor cells was observed (Figure 6a). This result indicates that HIF-1α expression in either tumor cells or hepatic normal cells or in both types of cells plays an important role in tumor progression. A histological study of the liver sections confirmed that the administration of pshHIF-1α significantly reduced the metastatic tumor growth in the liver (Figures 6c and d). Preadministration of pshHIF-1α reduced the tumor cell number in the liver at 12 days after tumor inoculation compared with the other groups (Figure 6b). This result implies that HIF-1α expression in the normal cells in the liver might play an important role in tumor cell growth in the liver, although the reduction

in the tumor cell number was modest compared with the case where the pshHIF-1α was administered after tumor inoculation. As demonstrated in our previous study, hydrodynamic delivery of pDNA can deliver pDNA to tumor cells in the liver. Moreover, we and other groups have reported that intratumoral expression of HIF-1α helps cancer cell survival and proliferation as well as angiogenesis and cancer metastasis. Therefore, hydrodynamic administration of pshHIF-1α could suppress HIF-1α expression in tumor cells, which might also act as an inhibitory treatment to prevent tumor progression. When HIF-1α expression is increased in normal cells, it might result in upregulation of genes that can assist tumor cell growth and progression. In the present study, we focused on MMP-9 as an HIF-1-dependent tumor supportive protein produced from normal cells. Normal cells, including hepatocytes, have significantly fewer genetic mutations than cancer cells. Therefore, inhibiting the increase in HIF-1α expression in hepatocytes would have less chance of inducing resistance to treatment.

In conclusion, this study suggests that HIF-1α expression is increased in normal liver cells as well as cancerous cells, and HIF-1α expression plays an important role in tumor progression. RNAi of HIF-1 is an effective strategy for inhibiting tumor cell growth, and both tumor and normal cells can be targets for RNAi-based anticancer treatment.

Materials and methods

Plasmid DNA

Short hairpin-expressing pDNAs targeting GFP or HIF-1α were constructed from piGENE hU6 vector (iGENE Therapeutics, Tsukuba, Japan) as described previously.[18] Target sites in GFP and murine HIF-1α genes are as follows: GFP, 5′-GGCTACGTCCAGGAGCGCA-3′ and HIF-1α, 5′-GACACAGCCTCGATATGAA-3′. These pDNAs transcribe a stem-loop-type RNA with a loop sequence of ACGUGUGCUGUCCGU. In a previous study, we confirmed that transfection of pshHIF-1α suppresses the mRNA expression of HIF-1α in cultured cells.[13] piGENE hU6 vector, which transcribes a non-related sequence of RNA with partial duplex formation, was used as a control pDNA throughout the present study.

pDsRed2-N1 encoding red fluorescent protein Dsred2 was purchased from BD Biosciences Clontech (Palo Alto, CA, USA). pGL4.74[hRluc/TK] (phRL-TK) encoding sea pansy luciferase under the control of herpes simplex virus TK promoter was purchased from Promega (Madison, WI, USA). A HRE reporter plasmid encoding firefly luciferase (pLuc-HRE) was generated by subcloning nine copies of the HRE (5′-TACGTGCTGC-3′) from mouse erythropoietin enhancer into *Bgl*II/*Hind*III site of pLuc-MCS plasmid (Stratagene, La Jolla, CA, USA).

Each pDNA was amplified in the DH5α strain of *Escherichia coli* and purified by using a Qiagen Endofree Plasmid Giga Kit (Qiagen GmbH, Hilden, Germany).

Cell culture

A murine colon carcinoma cell line Colon26, obtained from the Cancer Chemotherapy Center of the Japanese Foundation for Cancer Research (Tokyo, Japan), and Colon26 cells that stably express firefly luciferase (Colon26/Luc)[29] were cultured in RPMI 1640 medium supplemented with 10% fetal bovine serum (FBS) and penicillin/streptomycin/L-glutamine at 37 °C and 5% CO_2. A murine melanoma cell line B16-BL6 cells[30], obtained from the Cancer Chemotherapy Center of the Japanese Foundation for Cancer Research, were cultured in Dulbecco's modified Eagle's minimum essential medium (DMEM; Nissui Pharmaceutical, Tokyo, Japan) supplemented with 10% FBS and penicillin/streptomycin/L-glutamine at 37 °C and 5% CO_2. To mimic hypoxic conditions and induce HIF-1α protein expression, cells were incubated with the culture medium supplemented with 100 μM $CoCl_2$.[31]

In vitro *transfection*

Tumor cells were plated on culture plates. After an overnight incubation, transfection of pDNA was carried out using Lipofectamine 2000 (Invitrogen, Carlsbad, CA, USA) according to the manufacturer's instructions. In brief, 1 μg pDNA was mixed with 3 μg Lipofectamine 2000 at a final concentration of 2 μg pDNA ml^{-1} dissolved in OPTI-MEM I (Invitrogen). The resulting complex was added to the cells and the cells were incubated with the complex for 4 h. Cells were washed with PBS and further incubated with the culture medium supplemented with or without 100 μM $CoCl_2$ for the indicated periods.

Detection of HIF-1α protein expression by western blotting and ELISA

At 24 h after transfection, total proteins were collected from Colon26 and B16-BL6 cells. For total protein extraction, cells were lysed in a lysis buffer containing 50 mM Tris (pH 7.4), 1% NP40, 0.25% Na-deoxycholate, 0.1% SDS, 150 mM NaCl, 1 mM EDTA, 1 mM PMSF, 1 mM NaF and 0.2% Sigma protease inhibitor cocktail (Sigma Aldrich, St Louis, MO, USA). The lysate was centrifuged at 13 000 *g* for 20 min at 4 °C and the supernatant was collected and used as a protein sample. Protein concentrations were determined using a Proteostain Protein Quantification Kit (Dojindo Molecular Technologies Inc., Tokyo, Japan).

For western blotting, 50 μg protein was diluted with a loading buffer, denatured at 95 °C for 3 min, and resolved by SDS-polyacrylamide gel electrophoresis (SDS-PAGE) (6.5% polyacrylamide) and transferred to a polyvinylidene fluoride membrane (Immobilon-P; Millipore Corp., Bedford, MA, USA) by semidry blotting with Transblot SD (Bio-Rad, Hercules, CA, USA). To avoid nonspecific binding, the membrane was incubated in 5% bovine serum albumin. Then HIF-1α protein was detected by a primary monoclonal mouse antibody against HIF-1α (1:500; Novus Biologicals, Littleton, CO, USA) and a secondary peroxidase-conjugated rabbit anti-mouse IgG antibody (1:2000; Amersham Biosciences Inc., Piscataway, NJ, USA). Protein bands were visualized by chemiluminescence on the ECL Plus protein detection system (Amersham Biosciences).

Concentrations of HIF-1α in the samples from tumor cells treated with or without $CoCl_2$ were measured by an ELISA kit (DuoSet IC; R&D Systems, Minneapolis, MN, USA) according to manufacturer's protocol.

HIF-1-dependent reporter gene expression assay

Tumor cells seeded on culture plates were transfected with pLuc-HRE (0.8 μg ml^{-1}), phRL-TK (0.2 μg ml^{-1}) and a control pDNA, pshHIF-1α or pshGFP (1 μg ml^{-1}) using Lipofectamine 2000 as described above. At 4 h after transfection, cells were washed with PBS and further incubated with the culture medium with or without 100 μM $CoCl_2$ for an additional 20 h. Then cells were lysed using Promega passive lysis buffer (Promega). Samples were mixed with dual-luciferase reporter system (Promega) and the chemiluminescence produced was measured in a luminometer (Lumat LB9507; EG and G Berthold, Bad Wildbad, Germany). The results were calculated as the activity of firefly luciferase relative to that of sea pansy luciferase to correct for differences in transfection efficiency. The ratios of $CoCl_2$-treated cells were normalized to give *x*-fold values relative to those of the corresponding untreated group.

Animals

Four-week-old male BALB/c mice (approximately 20 g body weight), purchased from Shizuoka Agricultural Cooperative Association (Shizuoka, Japan), were used in all experiments. All animal experiments were conducted in accordance with the principles and procedures outlined in the US National Institutes of Health Guide for the Care and Use of Laboratory Animals. The protocols for animal experiments were approved by the Animal Experimentation Committee of the Graduate School of Pharmaceutical Sciences of Kyoto University.

Hepatic metastasis of tumor cells

Colon26/Luc cells in an exponential growth phase were harvested by trypsinization and suspended in Hank's balanced salt solution (HBSS; Nissui Pharmaceutical). Under ether anesthesia, a midline abdominal incision was made to expose the portal vein, and 1×10^5 Colon26/Luc cells were injected into the portal vein. Then the opening was sutured and mice were allowed to recover. At 5 days after tumor inoculation, mice received an intravenous injection of pDNA at a dose of 2.5 mg kg^{-1} body weight. The intravenous injection was performed by the hydrodynamics-based procedure where pDNA dissolved in saline in a volume of 8% of the body weight was injected into the tail vein within less than 5 s using a 26-gauge needle.[32]

To evaluate the effect of HIF-1α expression in normal liver cells on the growth of tumor cells in the liver, mice received a hydrodynamic delivery of pDNA, followed by inoculation of tumor cells into the portal vein after an interval of 3 days.

To visualize the location of Colon26 cells in the liver, Colon26 cells labeled with a red fluorescent protein, DsRed, were used instead of Colon26/Luc cells. DsRed2-labeled Colon26 cells were prepared by transfecting cells with pDsRed2-N1, and inoculated into mice 24 h after transfection.

Immunofluorescent staining of HIF-1α

To visualize HIF-1α expression in cultured cells, immunofluorescent staining of HIF-1α was carried out. At 24 h after transfection, cells were fixed with 4% paraformaldehyde in PBS. The cell membrane was permeabilized by PBS containing 0.1% Triton X-100. After blocking with 10% FBS in PBS, cells were incubated with a monoclonal mouse antibody against HIF-1α (1:500; Novus Biologicals). After washing, Alexa Fluor 488 goat anti-mouse secondary antibody (1:600; Molecular Probes, Invitrogen) was added. Nuclear staining was performed using propidium iodide staining solution (50 μg ml^{-1} propidium iodide and 1 μg ml^{-1} RNase A in PBS). Slides were prepared using a SlowFade Antifade Kit (Molecular Probes). Samples were examined using a confocal laser microscope (MRC-1024; Bio-Rad).

For the detection of HIF-1α expression in the liver, mice under ether anesthesia were euthanized by cutting the vena cava, and the liver was gently infused with 2 ml saline through the portal vein to remove the remaining blood in the organ. The liver was then placed in Tissue-Tek OCT embedding compound (Sakura Finetechnical Co Ltd, Tokyo, Japan), frozen in liquid nitrogen, and stored in 2-methyl butanol at −80 °C until use. Frozen liver sections (8 μm thick) were obtained with a cryostat (Jung CM 3000; Leica Microsystems AG, Wetzlar, Germany) using a routine procedure. Sections were stained with HIF-1α-specific antibody by the same procedure as cultured cells except for the blocking process. Liver sections were blocked using the Vector M.O.M Immunodetection Kit (Vector Laboratories, Burlingame, CA, USA). Sections were examined using a confocal laser microscope. Relative areas of the HIF-1α expression (green signal) to the total area in the images were quantitatively analyzed by using a BZ-Analyzer software (KEYENCE, Osaka, Japan).

Gelatin zymography

At 3 or 8 days after tumor inoculation, mice under ether anesthesia were euthanized by cutting the vena cava. The liver was gently infused with 2 ml saline through the portal vein to remove the remaining blood. The liver was excised and homogenized in 5 ml g^{-1} lysis buffer (0.1 M Tris (pH 7.8), 0.05% Triton-X-100). The homogenate was centrifuged at 13 000 *g* for 20 min at 4 °C, then the supernatant was collected. For the measurement of gelatinase activity, 500 μg protein was electrophoresed under non-reducing conditions on 10% SDS-polyacrylamide gel containing 0.1% gelatin. Gels were washed twice for 30 min in 2.5% Triton X-100 and once for 30 min in 10 mM Tris-HCl (pH 8.0) and incubated overnight in 50 mM Tris-HCl (pH 8.0) containing 10 mM $CaCl_2$ and 10 nM $ZnCl_2$. The gels were then stained with 0.2% Coomasie brilliant blue and destained in 5% methanol and 7% acetic acid.

VEGF ELISA assay

To determine VEGF production in culture supernatants *in vitro*, tumor cells seeded on culture plates were transfected as described above and supernatants were collected for ELISA 48 h after the transfection. VEGF protein levels in the supernatant were measured using mouse VEGF-specific ELISA (Quantikine; R&D systems).

Inhibitory effect of pshHIF-1α on tumor growth in the liver

At 12 days after tumor inoculation, mice were euthanized by cervical dislocation and the liver was excised and homogenized in a lysis buffer (0.1 M Tris (pH 7.8), 0.05% Triton X-100, 2 mM EDTA), and centrifuged at

13 000 *g* for 20 min at 4 °C. The supernatant was mixed with a luciferase assay buffer (Picagene; Toyo Ink, Tokyo, Japan), and the light produced was measured with a luminometer (Lumat LB 9507). The luciferase activity of the liver was converted to the number of Colon26/Luc cells using a regression line as previously reported.[29] Different sets of mice were used for the histological evaluation of tumor-bearing livers. At 12 days after tumor inoculation, frozen liver sections were made as described above and stained with hematoxylin and eosin, followed by an examination using a microscope (Biozero BZ-8000; KEYENCE).

Statistical analysis

Experiments were performed at least in duplicate, and a typical set of data was indicated. Differences were statistically evaluated by Student's *t*-test. A *P*-value of less than 0.05 was considered to be statistically significant.

Acknowledgements

This study was supported in part by Grants-in-Aid for Scientific Research from the Ministry of Education, Science, Sports, and Culture of Japan, by grants from the Ministry of Health, Labour and Welfare of Japan and by a Grant-in-Aid for Exploratory Research from the Japan Society for the Promotion of Sciences.

References

1 Fidler IJ. Critical determinants of metastasis. *Semin Cancer Biol* 2002; **12**: 89–96.
2 Weigelt B, Peterse JL, van't Veer LJ. Breast cancer metastasis: markers and models. *Nat Rev Cancer* 2005; **5**: 591–602.
3 Engers R, Gabbert HE. Mechanisms of tumor metastasis: cell biological aspects and clinical implications. *J Cancer Res Clin Oncol* 2000; **126**: 682–692.
4 Olaso E, Santisteban A, Bidaurrazaga J, Gressner AM, Rosenbaum J, Vidal-Vanaclocha F. Tumor-dependent activation of rodent hepatic stellate cells during experimental melanoma metastasis. *Hepatology* 1997; **26**: 634–642.
5 Liotta LA, Kohn EC. The microenvironment of the tumour–host interface. *Nature* 2001; **411**: 375–379.
6 Wang GL, Semenza GL. General involvement of hypoxia-inducible factor 1 in transcriptional response to hypoxia. *Proc Natl Acad Sci USA* 1993; **90**: 4304–4308.
7 Wenger RH. Cellular adaptation to hypoxia: O_2-sensing protein hydroxylases, hypoxia-inducible transcription factors, and O_2-regulated gene expression. *FASEB J* 2002; **16**: 1151–1162.
8 Salceda S, Caro J. Hypoxia-inducible factor 1alpha (HIF-1alpha) protein is rapidly degraded by the ubiquitin–proteasome system under normoxic conditions. Its stabilization by hypoxia depends on redox-induced changes. *J Biol Chem* 1997; **272**: 22642–22647.
9 Semenza GL. Targeting HIF-1 for cancer therapy. *Nat Rev Cancer* 2003; **3**: 721–732.
10 Zhong H, De Marzo AM, Laughner E, Lim M, Hilton DA, Zagzag D *et al*. Overexpression of hypoxia-inducible factor 1alpha in common human cancers and their metastases. *Cancer Res* 1999; **59**: 5830–5835.
11 Talks KL, Turley H, Gatter KC, Maxwell PH, Pugh CW, Ratcliffe PJ *et al*. The expression and distribution of the hypoxia-inducible factors HIF-1alpha and HIF-2alpha in normal human tissues, cancers, and tumor-associated macrophages. *Am J Pathol* 2000; **157**: 411–421.
12 Li L, Lin X, Staver M, Shoemaker A, Semizarov D, Fesik SW *et al*. Evaluating hypoxia-inducible factor-1alpha as a cancer therapeutic target via inducible RNA interference *in vivo*. *Cancer Res* 2005; **65**: 7249–7258.
13 Takahashi Y, Nishikawa M, Takakura Y. Suppression of tumor growth by intratumoral injection of short hairpin RNA-expressing plasmid DNA targeting beta-catenin or hypoxia-inducible factor 1alpha. *J Control Release* 2006; **116**: 90–95.
14 Elbashir SM, Harborth J, Lendeckel W, Yalcin A, Weber K, Tuschl T. Duplexes of 21-nucleotide RNAs mediate RNA interference in cultured mammalian cells. *Nature* 2001; **411**: 494–498.
15 Brummelkamp TR, Bernards R, Agami R. A system for stable expression of short interfering RNAs in mammalian cells. *Science* 2002; **296**: 550–553.
16 McCaffrey AP, Meuse L, Pham T-TT, Conklin DS, Hannon GJ, Kay MA. RNA interference in adult mice. *Nature* 2002; **418**: 38–39.
17 Song E, Lee SK, Wang J, Ince N, Ouyang N, Min J *et al*. RNA interference targeting Fas protects mice from fulminant hepatitis. *Nat Med* 2003; **9**: 347–351.
18 Takahashi Y, Nishikawa M, Kobayashi N, Takakura Y. Gene silencing in primary and metastatic tumors by small interfering RNA delivery in mice: quantitative analysis using melanoma cells expressing firefly and sea pansy luciferases. *J Control Release* 2005; **105**: 332–343.
19 Carroll VA, Ashcroft M. Role of hypoxia-inducible factor (HIF)-1alpha versus HIF-2alpha in the regulation of HIF target genes in response to hypoxia, insulin-like growth factor-I, or loss of von Hippel–Lindau function: implications for targeting the HIF pathway. *Cancer Res* 2006; **66**: 6264–6270.
20 Mazure NM, Brahimi-Horn MC, Berta MA, Benizri E, Bilton RL, Dayan F *et al*. HIF-1: master and commander of the hypoxic world. A pharmacological approach to its regulation by siRNAs. *Biochem Pharmacol* 2004; **68**: 971–980.
21 Kawabata K, Takakura Y, Hashida M. The fate of plasmid DNA after intravenous injection in mice: involvement of scavenger receptors in its hepatic uptake. *Pharm Res* 1995; **12**: 825–830.
22 Nishikawa M, Tamada A, Hyoudou K, Umeyama Y, Takahashi Y, Kobayashi Y *et al*. Inhibition of experimental hepatic metastasis by targeted delivery of catalase in mice. *Clin Exp Metastasis* 2004; **21**: 213–221.
23 Elezkurtaj S, Kopitz C, Baker AH, Perez-Cantó A, Arlt MJ, Khokha R *et al*. Adenovirus-mediated overexpression of tissue inhibitor of metalloproteinases-1 in the liver: efficient protection against T-cell lymphoma and colon carcinoma metastasis. *J Gene Med* 2004; **6**: 1228–1237.
24 Krishnamachary B, Berg-Dixon S, Kelly B, Agani F, Feldser D, Ferreira G *et al*. Regulation of colon carcinoma cell invasion by hypoxia-inducible factor 1. *Cancer Res* 2003; **63**: 1138–1143.
25 Shi YF, Fong CC, Zhang Q, Cheung PY, Tzang CH, Wu RS *et al*. Hypoxia induces the activation of human hepatic stellate cells LX-2 through TGF-beta signaling pathway. *FEBS Lett* 2007; **581**: 203–210.
26 Stuelten CH, DaCosta Byfield S, Arany PR, Karpova TS, Stetler-Stevenson WG, Roberts AB. Breast cancer cells induce stromal fibroblasts to express MMP-9 via secretion of TNF-alpha and TGF-beta. *J Cell Sci* 2005; **118**: 2143–2153.
27 Waas ET, Wobbes T, Lomme RM, DeGroot J, Ruers T, Hendriks T. Matrix metalloproteinase 2 and 9 activity in patients with colorectal cancer liver metastasis. *Br J Surg* 2003; **90**: 1556–1564.
28 Lakka SS, Rajan M, Gondi C, Yanamandra N, Chandrasekar N, Jasti SL *et al*. Adenovirus-mediated expression of antisense MMP-9 in glioma cells inhibits tumor growth and invasion. *Oncogene* 2002; **21**: 8011–8019.
29 Kuramoto Y, Nishikawa M, Hyoudou K, Yamashita F, Hashida M. Inhibition of peritoneal dissemination of tumor cells by single dosing of phosphodiester CpG oligonucleotide/cationic liposome complex. *J Control Release* 2006; **115**: 226–233.

30 Poste G, Doll J, Hart IR, Fidler IJ. *In vitro* selection of murine B16 melanoma variants with enhanced tissue-invasive properties. *Cancer Res* 1980; **40**: 1636–1644.
31 Gray MJ, Zhang J, Ellis LM, Semenza GL, Evans DB, Watowich SS *et al*. HIF-1alpha, STAT3, CBP/p300 and Ref-1/APE are components of a transcriptional complex that regulates Src-dependent hypoxia-induced expression of VEGF in pancreatic and prostate carcinomas. *Oncogene* 2005; **24**: 3110–3120.
32 Liu F, Song Y, Liu D. Hydrodynamics-based transfection in animals by systemic administration of plasmid DNA. *Gene Ther* 1999; **6**: 1258–1266.

Available online at www.sciencedirect.com
ScienceDirect
Journal of Biotechnology 133 (2008) 36–41
Journal of BIOTECHNOLOGY
www.elsevier.com/locate/jbiotec

Insertion of nuclear factor-κB binding sequence into plasmid DNA for increased transgene expression in colon carcinoma cells

Oranuch Thanaketpaisarn[a], Makiya Nishikawa[b,*], Takayuki Okabe[a], Fumiyoshi Yamashita[a], Mitsuru Hashida[a]

[a] *Department of Drug Delivery Research, Graduate School of Pharmaceutical Sciences, Kyoto University, Sakyo-ku, Kyoto 606-8501, Japan*
[b] *Department of Biopharmaceutics and Drug Metabolism, Graduate School of Pharmaceutical Sciences, Kyoto University, Sakyo-ku, Kyoto 606-8501, Japan*

Received 14 May 2007; received in revised form 20 August 2007; accepted 25 August 2007

Abstract

To increase plasmid DNA (pDNA)-based transgene expression, 5, 10 or 20 repeats of nuclear factor κB (NF-κB) binding sequences were inserted upstream of the cytomegalovirus (CMV) promoter region of a conventional pDNA encoding firefly luciferase (pCMV-Luc) to obtain pCMV-κB5-Luc, pCMV-κB10-Luc and pCMV-κB20-Luc. Murine carcinoma colon 26 cells, in which NF-κB was constitutively activated, were co-transfected with a firefly luciferase-expressing pDNA and a renilla luciferase-expressing pDNA having no NF-κB binding sequences using cationic liposomes. The expression efficiency of pCMV-κB(*n*)-Luc was evaluated using the ratio of the luciferase activities. Increasing numbers of NF-κB binding sequences significantly increased transgene expression. The expression was increased by NF-κB activators and the effects were marked with pDNA having many NF-κB binding sequences. These results indicate that insertion of NF-κB binding sequences into pDNA is an effective approach to increase transgene expression in cancer cells in which NF-κB is activated.
© 2007 Elsevier B.V. All rights reserved.

Keywords: Gene transfer; Transcription factor; Nuclear factor-κB; Reactive oxygen species; Colon carcinoma cell; Nuclear transport

1. Introduction

The final delivery barrier in plasmid DNA (pDNA)-mediated gene transfer is the passage through the nuclear membrane. Because the threshold size for DNA to freely pass through the nuclear pore complex (NPC) is a molecular weight of about 50 kDa, or between 200 and 310 bp in length (Ludtke et al., 1999). pDNA is generally too large to pass, unassisted, through the NPC. Therefore, pDNA is believed to enter the nucleus when the nuclear membrane structure disappears during the M-phase of mitosis (Moritimer et al., 1999; Tseng et al., 1999). Nuclear translocation has been reported to be the rate-limiting step in the gene transfer process rather than the cell entry (Zhou et al., 2004). Lack of an efficient translocation of pDNA into the nucleus through the NPC, where it is transcribed, results in unacceptably low levels of transgene expression by most nonviral gene transfer methods. Nonviral vectors, such as cationic lipids (liposomes) and polymers, could protect pDNA from nuclease degradation, and improve its cellular entry, but they may not assist pDNA in its nuclear entry, because pDNA is eventually released from the complexes before entering the nucleus (Zabner et al., 1995; Xu and Szoka, 1996).

Dean et al. demonstrated that any eukaryotic promoter, enhancer, insulator, or regulatory specific sequence plays important roles in the nuclear targeting of DNA (Dean et al., 2005); following cytoplasmic microinjection, pDNA is translocated into the nucleus in association with several types of transcription factors (Dean, 1997; Dean et al., 1999). One of the most important transcription factors in the nuclear entry of pDNA is nuclear factor κB (NF-κB). NF-κB protein localizes in the cytoplasm in a bound form with its inhibitory protein, IκB, which shields the nuclear localization signal of NF-κB. Once cells are exposed to any signal that activates NF-κB, specific IκB family members rapidly undergo stimulus-coupled phosphorylation,

Abbreviations: pDNA, plasmid DNA; NF-κB, nuclear factor κB; NPC, nuclear pore complex; ROS, reactive oxygen species; CMV, cytomegalovirus; PMS, phenazine methosulfate.

* Corresponding author. Tel.: +81 75 753 4580; fax: +81 75 753 4614.
E-mail address: makiya@pharm.kyoto-u.ac.jp (M. Nishikawa).

0168-1656/$ – see front matter © 2007 Elsevier B.V. All rights reserved.
doi:10.1016/j.jbiotec.2007.08.047

ubiquitination and proteasome-mediated degradation, resulting in the liberation of active NF-κB heterodimers. After entering the nucleus, the activated NF-κB can bind specifically to its corresponding NF-κB binding sequence in DNA, leading to enhanced transcription and expression of downstream genes (Pahl, 1999). It has also been reported that pDNA can be translocated into the nucleus by inserting NF-κB binding sequences (Mesika et al., 2001). In a previous study, we demonstrated that an intravenous injection of pDNA/cationic liposome complex (lipoplex) activated the NF-κB in mouse lung, and this activation can be used to enhance lipoplex-mediated transgene expression by inserting NF-κB binding sequences into pDNA (Kuramoto et al., 2006).

These pieces of evidence suggest that the NF-κB activity of cells, which is a function of various physiological conditions, influences the level of transgene expression by pDNA-based gene transfer. Abnormally high NF-κB activity can be found in affected organs of patients with rheumatoid arthritis, asthma and inflammatory bowel disease (Kumar et al., 2004), as well as in acute lymphoblastic leukemia, breast cancer and diverse solid tumor-derived cell lines (Visconti et al., 1997). NF-κB is generally thought to be involved in the primary oxidative stress–response, acting as a redox-sensitive transcription factor. Reactive oxygen species (ROS) can function as components of signal transduction cascades in many cellular processes and act as common second messengers following cellular exposure to agents that induce NF-κB activation (Gius et al., 1999). ROS, such as hydrogen peroxide, have been reported to induce NF-κB activation in some types of cells (Mercurio and Manning, 1999; Bowie and O'Neill, 2000) and are signal molecules that play important roles in tumor growth and metastasis (Zhu et al., 2002; Rhee, 1999; Yoon et al., 2002).

In this study, to increase the transgene expression by nonviral vectors for cancer gene therapy, we first examined whether NF-κB is activated in colon carcinoma cells and whether this activation can be further increased by the treatment of cells with phenazine methosulfate (PMS) or hydrogen peroxide. Then, we designed new pDNA constructs by inserting NF-κB binding sequences to a conventional pDNA and examined whether the addition of the sequences is effective in increasing transgene expression. We propose here that the insertion of a suitable number of NF-κB binding sequences into pDNA is an effective approach to increasing transgene expression in cells in which NF-κB is transiently or constitutively activated.

2. Materials and methods

2.1. Chemicals

PathDetect® NF-κB *cis*-reporting pNF-κB-Luc plasmid was purchased from Stratagene (La Jolla, CA). Plasmid DNA encoding renilla luciferase under the control of SV40 promoter (pSV40-RL) was purchased from Promega (Madison, WI). Oligonucleotides were purchased from Nihon Gene Research (Sendai, Japan); a pair with a consensus NF-κB binding sequence (5′-TCAGAGGGGACTTTCCGAGAGG-3′ and 3′-AGTCTCCCCTGAAAGGCTCTCC-5′, the underlined part represents an NF-κB binding sequence) and another pair without the binding sequence (5′-AGTGTCAGCACGTGGAGATGCG-3′ and 3′-TCACAGTCGTGCACCTCTACGC-5′). [γ-^{32}P]ATP was purchased from Amersham (Tokyo, Japan). Lipofectamine2000 was purchased from GIBCO-Invitrogen (Carlsbad, CA). Opti-MEM® was obtained from Gibco BRL (Grand Island, NY). Dual-Luciferase™ Reporter Assay was purchased from Wako Pure Chemical (Osaka, Japan). All other chemicals were of the highest purity available.

2.2. Preparation of pDNA constructs

pCMV-Luc was constructed by inserting the firefly luciferase cDNA fragment from pGL3-control vector (Promega, Madison, WI) into the HindIII/XbaI site of pcDNA3 vector (Invitrogen, Carlsbad, CA) as previously reported (Sakurai et al., 2001). pCMV-κB(n)-Luc (n = 5, 10 or 20) was constructed as follows. The five repeats of the NF-κB binding sequence were amplified from pNF-κB-Luc by PCR using a set of primers (5′-primer, GAAGATCTATGTCTGGATCCAAGCTA; 3′-primer, TGTTCGCGAATACCCTCTAGAGTCACC) containing the BglII (5′-end) and NruI (3′-end) site, then the PCR product was digested with the restriction enzymes. Then, the DNA fragment was cloned into the BglII/NruI site of pCMV-Luc to obtain pCMV-κB5-Luc as reported previously (Kuramoto et al., 2006). To construct pCMV-κB10-Luc, the five repeats of the NF-κB binding sequence were amplified from pCMV-κB5-Luc with a set of primers (5′-primer, TGTTCGCGAATGTCTGGATCCAAGCTA; 3′-primer, GGTGACTCTAGAGGGTATGGATCCCG) containing the BamHI site and the BamHI-digested fragment was inserted into the BamHI site of pCMV-κB5-Luc. The 10 repeats of the NF-κB binding sequence were amplified from pCMV-κB10-Luc with a set of primers (5′-primer, TGTTCGCGAGTCGACGGATCGGGAGATCT; 3′-primer, ATCTGGCCCGTACATCGCGA) containing NruI sites and the NruI-digested fragment was inserted into the NruI site of pCMV-κB10-Luc to obtain pCMV-κB20-Luc. The sequences of these pDNA preparations were confirmed by automated sequencing. Fig. 1 shows the schematic presentation of these pDNA constructs. Each pDNA was amplified in *E. coli* strain DH5α, then isolated and purified using a Qiagen Endofree™ Plasmid Giga Kit (Qiagen GmbH, Hilden, Germany). The lipopolysaccharide concentration in a pDNA sample was estimated with a LAL assay kit (Limus F Single Test Wako; Wako Pure Chemical, Osaka, Japan) and found to be less than 22 pg/μg DNA. Then, purified pDNA was dissolved in a sterilized endotoxin-free 5% dextrose solution and stored at −20 °C until use.

2.3. In vitro transfection and reporter gene assay

Mouse colon carcinoma colon 26 cells were maintained in RPMI-1640 (Life Technologies Gibco BRL) supplemented with 10% heat-inactivated FBS, penicillin G (100 U/ml) and streptomycin (100 μg/ml) and 4 mM L-glutamine at 37 °C in a 5% CO_2/air humidified atmosphere. Cells were plated on 12-well culture plates at a density of 3×10^5 cells per well

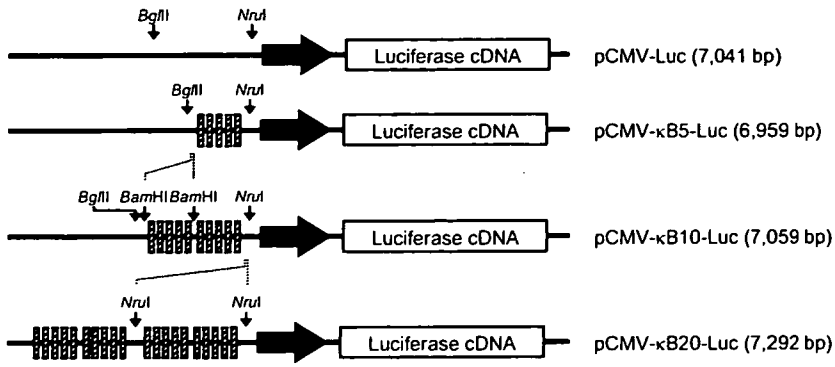

Fig. 1. Schematic presentation of pDNA encoding firefly luciferase cDNA under the control of the human CMV immediate early promoter (black arrow). Each striped box indicates an NF-κB binding sequence (5′-GGGGACTTTCC-3′). The numbers in parentheses indicate the size of each pDNA.

and incubated for 24 h prior to transfection. A pDNA (0.5 μg) encoding firefly luciferase, i.e., pCMV-Luc or pCMV-κB(*n*)-Luc (*n* = 5, 10 or 20), and pRL-SV40 (0.1 μg) were complexed with 1.8 μg LipofectAMINE™2000 (GIBCO-Invitrogen) in 1 ml Opti-MEM. The lipoplex formed was added to the cells and incubated for 4 h. Cells were incubated with PMS (1 or 2 μM) or hydrogen peroxide (100 μM) for 10 h. At 22 h after transfection, the cells were scraped off into a lysis buffer (0.1 M Tris, 0.05% Triton X-100, 2 mM EDTA, pH 7.8), transferred to a 1.5 ml tube and subjected to three cycles of freezing in liquid nitrogen for 3 min and thawing in a water bath at 37 °C for 2 min. The homogenates were centrifuged at 10,000 × g for 8 min at 4 °C. Then, 10 μl of the supernatant was mixed with 100 μl luciferase assay buffer for luciferase assay and then 100 μl of renilla assay buffer was added to the same tube for the renilla assay using the Dual-Luciferase™ Reporter Assay kit (Promega, Madison, WI). The chemiluminescence was measured in a luminometer (Lumat LB 9507, EG&G Berthold, Bad Wildbad, Germany). The luciferase activities were measured and the expression efficiency of pCMV-Luc or pCMV-κB(*n*)-Luc was evaluated by calculating the ratio of the firefly/renilla luciferase activities. The renilla luciferase was used to normalize any experimental variations among samples, such as transfection efficiency.

2.4. Preparation of nuclear protein extracts

The nuclear protein extracts were collected from colon 26 cells using a nuclear extract kit (Active motif, CA). The concentration of nuclear protein in the supernatant of the extract was determined with the Protein Quantification Kit-Wide range (Dojindo Molecular Technologies Inc., Kumamoto, Japan). To activate NF-κB, colon 26 cells were treated with 4 μM PMS, and the nuclear protein extracts were collected as described above.

2.5. Electrophoretic mobility shift assay (EMSA)

EMSA was performed as described previously (Zhou et al., 1999). The oligonucleotide containing an NF-κB binding sequence and its antisense oligonucleotide were separately end-labeled with [γ-^{32}P]ATP using polynucleotide kinase T4 (MEGALABEL™, Takara Bio Inc, Otsu, Japan). Both end-labeled oligonucleotides were purified from unincorporated [γ-^{32}P]ATP using a Sephadex G-50 column (Pharmacia, Uppsala, Sweden) and recovered in TNE buffer (10 mM Tris–HCl, 0.1 M NaCl, 1 mM EDTA, pH 7.5). The purified oligonucleotides were incubated for 10 min at room temperature for annealing to obtain the radiolabeled double-stranded DNA probe for EMSA. An aliquot of 60 μg extracted nuclear protein was incubated with a binding buffer (20 mM Hepes, pH 7.9, 0.5 mM EDTA, pH 8.0, 50 mM KCl, 10% glycerol, 0.5 mM DTT, 0.5 mM PMSF) and 2 μg salmon sperm DNA for 15 min on ice. Then, 1.5 × 10^6 cpm of the radiolabeled double-stranded DNA probe was added to the sample followed by an additional 30 min incubation at 4 °C. Two microliters 0.1% bromphenol blue dye was used as a marker. An aliquot of 20 μl of the resulting solution was electrophoresed on a 4% nondenaturing polyacrylamide gel for 90 min at 150 V in TBE buffer in a cold room. After completion of the electrophoresis, the gel was transferred to a piece of blotting paper and dried under vacuum. The dried gel was exposed to an Imaging Plate (Fuji Photo Film, Kanagawa, Japan) and analyzed using a Bio-Image Analyzer System (BAS-2500, Fuji Photo Film). The specificity of the observed signals was also confirmed by using the unlabeled double-strand DNA without any NF-κB binding sequence.

2.6. Statistical analysis

Differences were statistically evaluated by one-way ANOVA followed by the Student-Newmann–Keuls multiple comparison test using SPSS software, and the level of statistical significance was $P < 0.05$.

3. Results

3.1. NF-κB activity in colon carcinoma cells

NF-κB activity was detected by EMSA. The nuclear fractions of colon carcinoma cells were subjected to electrophoresis using ^{32}P-labeled double-stranded oligonucleotides having an NF-κB binding sequence. A band representing the presence of proteins that bind to the DNA probe was detected in the nuclear fraction of colon 26 cells under normal culture conditions (Fig. 2, lane 1), suggesting that NF-κB is constitutively activated in the

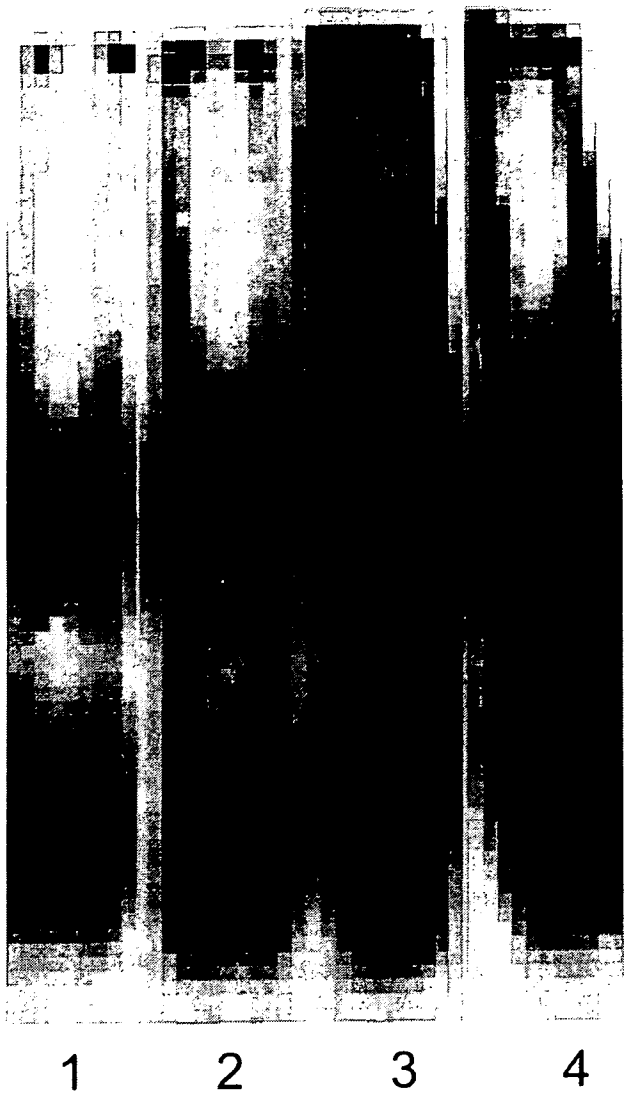

Fig. 2. EMSA analysis of nuclear NF-κB in colon 26 cells. Nuclear proteins extracted from colon 26 cells were analyzed using double-stranded oligonucleotides containing an NF-κB binding sequence (5′-TCAGAGGGGACTTTCCGAGAGG-3′) end-labeled with [γ-^{32}P]ATP. Lane 1, untreated cells. Lanes 2–4, PMS (4 μM), treated cells for 10 h, followed by 0 h (lane 2), 3 h (lane 3), or 10 h (lane 4) incubation in PMS-free medium.

proliferating colon 26 cells. The amount of nuclear NF-κB was increased by PMS treatment (Fig. 2, lane 2). In addition, the activation of NF-κB was also observed at 3 and 10 h after treatment (Fig. 2, lanes 3, and 4, respectively). These results indicate that ROS, which are generated by PMS, activate NF-κB in colon 26 cells, and that the activation lasts for at least 10 h after removal of PMS.

3.2. Increased transgene expression by increasing NF-κB binding sequences in pDNA

Fig. 3 shows the transgene expression in colon 26 cells after transfection of pCMV-Luc, pCMV-κB5-Luc, pCMV-κB10-Luc or pCMV-κB20-Luc. Under control conditions, pCMV-κB5-Luc produced a 1.74-fold increase in transgene expression in colon 26 cells compared with pCMV-Luc ($P < 0.05$). Increasing the number of the NF-κB binding sequences to 10 or 20 further increased the expression ($P < 0.05$ against pCMV-Luc or pCMV-κB5-Luc). A positive correlation between the number of NF-(B binding sequences added and transgene expression was observed ($R^2 = 0.938$). However, the expression almost reached a plateau level when the number of sequence added was 10, and there was no statistically significant difference between the expression levels of pCMV-κB10-Luc and pCMV-κB20-Luc.

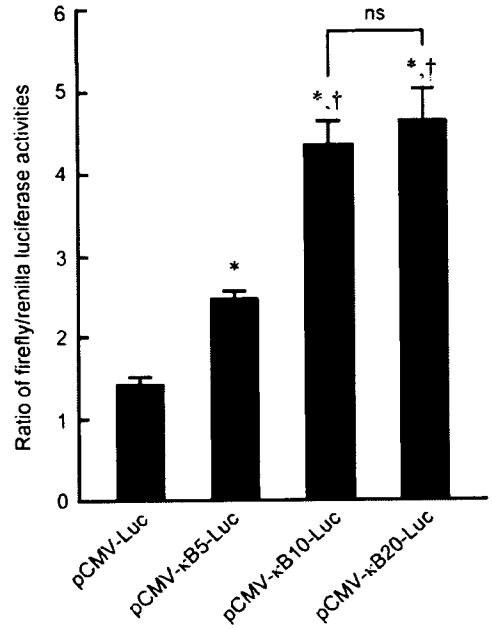

Fig. 3. Transgene expression in colon 26 cells by pCMV-Luc and pCMV-κB(*n*)-Luc ($n = 5$, 10 or 20). Colon 26 cells were transfected with lipoplex consisting of one of the firefly luciferase-expressing pDNAs (0.5 μg per well) and pRL-SV40 (0.1 μg per well) for 4 h. At 22 h after transfection, firefly and renilla luciferase activities were measured and expressed as the ratio of these activities (mean ± S.D.). *A statistically significant difference ($P < 0.05$) compared with pCMV-Luc; †a statistically significant difference ($P < 0.05$) compared with pCMV-κB5-Luc; ns, not significant.

3.3. Effects of PMS on transgene expression in colon carcinoma cells

Fig. 4A shows the transgene expression by pCMV-Luc or pCMV-κB(*n*)-Luc in colon 26 cells treated with different concentration of PMS. With any pDNA, the addition of PMS, which generates superoxide anion and hydrogen peroxide, increased the transgene expression in a PMS concentration-dependent manner. Similar results were obtained when the cells were treated with hydrogen peroxide (data not shown). However, under all the conditions examined, pDNA with many NF-κB binding sequences showed higher transgene expression than those with fewer. These results clearly indicate that the novel pDNAs with 10 or 20 NF-κB binding sequences are effective in achieving high transgene expression in cells where NF-κB is highly activated. Linear correlations were observed between the

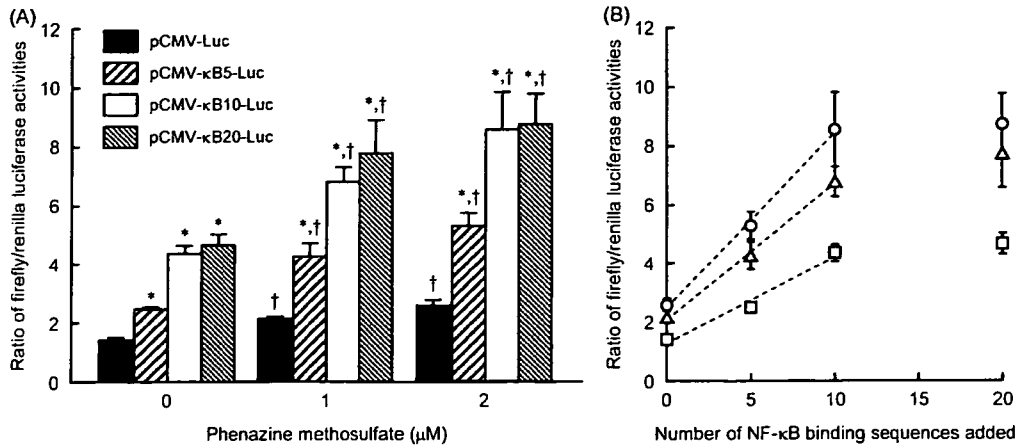

Fig. 4. (A) Effect of PMS on transgene expression in colon 26 cells. Colon 26 cells were transfected with lipoplex consisting of one of the firefly luciferase-expressing pDNAs (0.5 μg per well) and pRL-SV40 (0.1 μg per well) for 4 h. PMS (1 or 2 μM) was added and incubated for 10 h. At 22 h after transfection, firefly and renilla luciferase activities were detected and expressed as the ratio of these activities (mean ± S.D.). *A statistically significant difference ($P < 0.05$) compared with the pCMV-Luc group; †a statistically significant difference ($P < 0.05$) compared with the no treatment group. (B) Relationship between the transgene expression and the number of NF-κB binding sequences added to pCMV-Luc. Experimental details are described in the legend of (A). The dashed regression lines were obtained using the data, except for those of pCMV-κB20-Luc, and the slopes are 0.29, 0.46 and 0.60 for PMS concentrations of 0 μM (□), 1 (Δ) and 2 μM (○), respectively. Results are expressed as the ratio of the firefly/renilla luciferase activities (mean ± S.D.).

number of NF-κB binding sequences added and the increase in the transgene expression when the number of the NF-κB sequences was 10 or fewer (Fig. 4B). The slope of the regression line became steeper as the PMS concentration increased, suggesting that the advantage of the novel pDNA with many NF-κB binding sequences over a conventional pDNA is marked when the NF-κB in target cells is highly activated.

4. Discussion

Plasmid DNA is unlikely to passively diffuse into the nucleus because its size is much greater than the passive diffusion limit (40–60 kDa) (Ohno et al., 1998). Microinjection of pDNA fragments >2000 bp in length, or any macromolecule >2000 kDa also results in little diffusion into the cytoplasm (Dowty et al., 1995; Lukacs et al., 2000). When pDNA migrates from the cytoplasm to the nucleus, except during mitosis, it must pass through the NPC that is present in the nuclear envelope (Dean et al., 1999). Macromolecules that use the NPC pathway have to be provided with a nuclear localization signal (NLS). However, pDNA does not have any such signals, so this suggests that there may be a certain substance that provides pDNA with NLS. It has been postulated by Dean that binding of transcription factors to their corresponding sequences in pDNA leads to nuclear transport of pDNA through the NPC (Dean et al., 1999). Mesika also reported NF-κB-assisted importation of pDNA into the nuclei of mammalian cells (Mesika et al., 2001). The association of NLS, NF-κB p50, to pDNA not only enhanced the passage of pDNA across the NPC but also facilitated its transport in the cytoplasm (Mesika et al., 2005). Furthermore, we demonstrated by competitive EMSA that the insertion of five repeats of the NF-κB binding sequence into a conventional pDNA increases its binding to NF-κB nuclear protein, resulting in an increased transgene expression (Kuramoto et al., 2006). NF-κB is required for oncogenesis in multiple processes. In addition, some cancer cells depend on NF-κB for their survival (Baldwin, 2001). These findings suggested to us idea that activated NF-κB, which can be found in some cancer cells, can be used as a vehicle for pDNA to enter the nucleus if it contains NF-κB binding sequences. In a previous study, we demonstrated that the insertion of five repeats of the binding sequences into pDNA is effective in increasing the transgene expression in mouse lung after systemic injection as complexes with cationic liposomes. To examine the effect of the number of the binding sequences on transgene expression, we prepared three pDNA preparations in which 5, 10 or 20 additional NF-κB binding sequences were inserted.

The pDNA preparations having additional NF-κB binding sequences showed higher transgene expression than pCMV-Luc in colon 26 cells. There was a trend suggesting that the expression was proportional to the number of added NF-κB binding sequences. However, the expression level by pCMV-κB20-Luc was not significantly higher than that by pCMV-κB10-Luc, suggesting that 10–20 NF-κB binding sequences are optimal for increasing pDNA-based transgene expression. Griesenbach et al. reported that the addition of NF-κB decoy, which is a short double-stranded DNA with an NF-κB binding sequence, into pDNA complex with cationic liposomes reduced the inflammatory response to the complexes (Griesenbach et al., 2000). As demonstrated, NF-κB decoy may prevent the binding of activated NF-κB to its binding sequences in the genome or in pDNA. Because the number of activated NF-κBs is limited, more NF-κB binding sequences in pDNA may act as a decoy and prevent an increase in transgene expression. Ten to 20 NF-κB binding sequences seemed to be optimal for enhanced transgene expression under the present experimental conditions.

The amount of plasmids in the nuclear fraction of transfected cells was measured using real time PCR. A large amount of DNA was detected when the pCMV-κB5-Luc was used for

transfection (0.89 ± 0.07% of genome DNA) compared with the pCMV-Luc (0.72 ± 0.15%), although the difference was not statistically significant ($P = 0.2$) because of the large standard errors and small sample numbers ($n = 3$). These results could support the hypothesis that the nuclear transport is increased by the insertion of the binding sequences into plasmid DNA. However, the differences in transcription efficiency would also contribute to the expression efficiency, because the differences in the transgene expression were much greater than that in the amount of plasmids in the nuclear fraction. The activated NF-κB can bind specifically to its corresponding NF-κB binding sequence in DNA, leading to enhanced transcription and expression of downstream genes (Pahl, 1999). Therefore, the insertion of NF-κB binding sequences into plasmid DNA can increase the nuclear transport of the DNA and the transcription efficiency, both of which will contribute to the increased transgene expression of plasmid DNA with many numbers of the binding sequences.

As demonstrated with several cancer cells, NF-κB is constitutively activated in colon 26 cells under normal culture conditions. The addition of PMS, which is known to induce ROS (superoxide anion and H_2O_2) within cells, will further activate NF-κB. The expression by any pDNA construct was increased when the concentration of PMS added to the cells increased. These results indicate that the transgene expression by pDNA with NF-κB binding sequences is a function of the NF-κB activity of the cells.

In conclusion, we have successfully developed a novel pDNA in which additional NF-κB binding sequences were inserted. We have also clearly demonstrated that insertion of NF-κB binding sequences into plasmid DNA can improve the efficiency of pDNA-based gene transfer in cells where NF-κB activity is high. The level of transgene expression was found to be a function of the level of the NF-κB activity of cells. These results indicate that insertion of NF-κB binding sequences into pDNA is an effective approach to increase transgene expression in cancer cells in which NF-κB is activated

Acknowledgements

This work was supported in part by Grants-In-Aid for Scientific Research from the Ministry of Education, Culture, Sports, Science and Technology, Japan, and by grants from the Ministry of Health, Labour and Welfare, Japan.

References

Baldwin, A.S., 2001. Control of oncogenesis and cancer therapy resistance by the transcription factor NF-κB. J. Clin. Invest. 107, 241–246.

Bowie, A., O'Neill, L.A.J., 2000. Oxidative Stress and nuclear factor-κB activation: a reassessment of the evidence in the light of recent discoveries. Biochem. Pharmacol. 59, 13–23.

Dean, D.A., 1997. Import of plasmid DNA into the nucleus is sequence specific. Exp. Cell Res. 230, 293–301.

Dean, D.A., Dean, B.S., Muller, S., 1999. Sequence requirements for plasmid nuclear import. Exp. Cell Res. 253, 713–722.

Dean, D.A., Strong, D.D., Zimmer, W.E., 2005. Nuclear entry of nonviral vectors. Gene Ther. 12, 881–890.

Dowty, M.E., Williams, P., Zhang, G., Hagstrom, J.E., Wolff, J.A., 1995. Plasmid DNA entry into postmitotic nuclei of primary rat myotubes. Proc. Natl. Acad. Sci. U.S.A. 92, 4572–4576.

Gius, D., Botero, A., Shah, S., Curry, H.A., 1999. Intracellular oxidation/reduction status in the regulation of transcription factors NF-κB and AP-1. Toxicol. Lett. 106, 93–106.

Griesenbach, U., Scheid, P., Hillery, E., Martin, R., Huang, L., Geddes, D.M., Alton, E.W., 2000. Anti-inflammatory gene therapy directed at the airway epithelium. Gene Ther. 7, 306–313.

Kumar, A., Takada, Y., Boriek, A.M., Aggarwal, B.B., 2004. Nuclear factor-κB: its role in health and disease. J. Mol. Med. 82, 434–448.

Kuramoto, T., Nishikawa, M., Thanaketpaisarn, O., Okabe, T., Yamashita, F., Hashida, M., 2006. Use of lipoplex-induced nuclear factor-κB activation to enhance transgene expression by lipoplex in mouse lung. J. Gene Med. 8, 53–62.

Ludtke, J.J., Zhang, G., Sebestyen, M.G., Wolff, J.A., 1999. A nuclear localization signal can enhance both the nuclear transport and expression of 1 kb DNA. J. Cell Sci. 112, 2033–2041.

Lukacs, G.L., Haggie, P., Seksek, O., 2000. Size-dependent DNA mobility in cytoplasm and nucleus. J. Biol. Chem. 275, 1609–1625.

Mercurio, F., Manning, A.M., 1999. NF-κB as a primary regulator of the stress response. Oncogene 18, 6163–6171.

Mesika, A., Grigoreva, I., Zohar, M., 2001. A regulated NF-κB-assisted import of plasmid DNA into mammalian cell nuclei. Mol. Ther. 3, 653–657.

Mesika, A., Kiss, V., Brumfeld, V., Ghosh, G., Reich, Z., 2005. Enhanced intracellular mobility and nuclear accumulation of DNA plasmids associated with a karyophilic protein. Hum. Gene Ther. 16, 200–208.

Moritimer, I., Tam, P., MacLachlan, I., Graham, R.W., Saravolac, E.G., Joshi, P.B., 1999. Cationic lipid-mediated transfection of cells in culture requires mitotic activity. Gene Ther. 6, 403–411.

Ohno, M., Fornerod, M., Mattaj, I.W., 1998. Nucleocytoplasmic transport: the last 200 nanometers. Cell 92, 327–336.

Pahl, H.L., 1999. Activators and target genes of Rel/NF-κB transcription factors. Oncogene 18, 6853–6866.

Rhee, S.G., 1999. Redox signalling: hydrogen peroxide as intracellular messenger. Exp. Mol. Med. 35, 53–59.

Sakurai, F., Nishioka, T., Saito, H., Baba, T., Okuda, A., Matsumoto, O., Taga, T., Yamashita, F., Takakura, Y., Hashida, M., 2001. Interaction between DNA-cationic liposome complexes and erythrocytes is an important factor in systemic gene transfer via the intravenous route in mice: the role of the neutral helper lipid. Gene Ther. 8, 677–686.

Tseng, W.C., Haselton, F.R., Giorgio, T.D., 1999. Mitosis enhances transgene expression of plasmid delivered by cationic liposomes. Biochim. Biophys. Acta 1445, 53–64.

Visconti, R., Cerutti, J., Battista, S., Fedele, M., Trapasso, F., Zeki, K., Miano, M.P., Nigris de, F., Casalino, L., Curcio, F., Santoro, M., Fusco, A., 1997. Expression of the neoplastic phenotype by human thyroid carcinoma cell lines requires NF-κB p65 protein expression. Oncogene 15, 1987–1994.

Xu, Y., Szoka Jr., F.C., 1996. Mechanism of DNA release from cationic liposome/DNA complexes used in cell transfection. Biochemistry 35, 5616–5623.

Yoon, S.O., Park, S.J., Yoon, S.Y., Yun, C.H., Chung, A.S., 2002. Sustained production of H_2O_2 activates pro-matrix metalloproteinase-2 through receptor tyrosine kinases/phosphatidylinositol 3-kinase/NF-κB pathway. J. Biol. Chem. 277, 30271–30282.

Zabner, J., Fasbender, A.J., Moninger, T., Poellinger, K.A., Welsh, M.J., 1995. Cellular and molecular barriers to gene transfer by a cationic lipid. J. Biol. Chem. 270, 18997–19007.

Zhou, D., Brown, S.A., Yu, T., 1999. High dose of ionizing radiation induced tissue-specific activation of nuclear factor-κB *in vivo*. Radiat. Res. 151, 703–709.

Zhou, R., Geiger, R.C., Dean, D.A., 2004. Intracellular trafficking nucleic acids. Expert Opin. Drug Deliv. 1, 127–140.

Zhu, J.W., Yu, B.M., Ji, Y.B., Zhang, M.H., Li, D.H., 2002. Upregulation of vascular endothelial growth factor by hydrogen peroxide in human colon cancer. World J. Gastroenterol. 8, 153–157.

Int. J. Cancer: **121**, 401–406 (2007)
© 2007 Wiley-Liss, Inc.

Improved anti-cancer effect of interferon gene transfer by sustained expression using CpG-reduced plasmid DNA

Hiroki Kawano[1], Makiya Nishikawa[1], Masaru Mitsui[1], Yuki Takahashi[1], Keiko Kako[1], Kiyoshi Yamaoka[1], Yoshihiko Watanabe[2] and Yoshinobu Takakura[1]*

[1]*Department of Biopharmaceutics and Drug Metabolism, Graduate School of Pharmaceutical Sciences, Kyoto University, Sakyo-ku, Kyoto, Japan*

[2]*Department of Molecular Microbiology, Graduate School of Pharmaceutical Sciences, Kyoto University, Sakyo-ku, Kyoto, Japan*

Plasmid DNA (pDNA) expressing mouse interferon (IFN)-β or IFN-γ (pCMV-Muβ and pCMV-Muγ, respectively) has been shown to be effective in inhibiting the growth of colon carcinoma CT-26 cells in the liver (Kobayashi *et al.*, Molecular Therapy 2002;6:737–44). The therapeutic effect of such IFN gene transfer could be significantly increased by the sustained expression of IFNs. In the present study, CpG-reduced pDNA encoding IFN-β or IFN-γ (pGZB-Muβ and pGZB-Muγ, respectively) was constructed. pCMV-Muβ and pCMV-Muγ were used as conventional CpG-replete pDNAs. Each pDNA was injected into the tail vein of mice by the hydrodynamics-based procedure. An injection of pGZB-Muβ resulted in very high IFN-β activities in the serum for at least 24 hr after injection, whereas the IFN-β activity after pCMV-Muβ injection declined quickly. About a 14-fold greater amount of IFN-β was produced from pGZB-Muβ than from pCMV-Muβ. pGZB-Muβ markedly inhibited the pulmonary metastasis of CT-26 cells. Similar, but more marked results were obtained with pGZB-Muγ: it increased the area under the concentration-time curve by more than a 60-fold and the mean residence time of IFN-γ 4-fold compared with pCMV-Muγ. The survival time of the pGZB-Muγ-treated mice was significantly ($p < 0.05$) longer than that of the saline- or pCMV-Muγ-treated mice. These results indicate that long-term expression of IFN can be achieved by CpG-reduced pDNA and sustained IFN gene expression results in enhanced therapeutic effects of IFN gene transfer against tumor metastasis.
© *2007 Wiley-Liss, Inc.*

Key words: interferon; cancer gene therapy; pulmonary metastasis; hydrodynamics; CpG dinucleotides

High and sustained transgene expression is indispensable for effective gene therapy. Generally speaking, persistent gene expression increases the therapeutic benefits of gene transfer and reduces the need for redosing. Although plasmid DNA (pDNA), the most frequently-used nonviral vector, avoids the fatal disadvantages that have been experienced with viral vectors, such as virus-induced acute organ failure and insertional mutagenesis, its transgene expression characteristics need to be improved for effective *in vivo* gene therapy.[1,2] The low level of transgene expression has been unacceptable in pDNA-based nonviral vectors for many years, but the development of highly effective nonviral gene delivery methods has now almost solved the problem. The application of electric pulses or ultrasound can significantly increase the level of transgene expression up to 100-fold or more in various experimental settings. In addition Liu *et al.*[3] and Zhang *et al.*[4] have demonstrated that a very high level of transgene expression can be obtained by an intravenous injection of naked pDNA dissolved in a large volume of saline when injected at a high velocity: the so-called hydrodynamics-based procedure.[3] This method of gene delivery results in a high level of transgene expression in internal organs, particularly the liver, apparently unaccompanied by any severe toxicity.[5,6] Therefore, this method could be applied therapeutically with some modifications.[7] However, the transient nature of transgene expression by nonviral vectors is still a major problem associated with nonviral vector-based gene transfer.

Cytokine-supported tumor immunotherapy is a promising strategy for cancer gene therapy. Interferon (IFN) gene transfer is considered to be useful for immunotherapy because IFNs have antiproliferative and immunomodulatory activities which are capable of contributing to the host's defense against tumors.[8–11] We have reported that IFN-β or IFN-γ gene delivery by the hydrodynamics-based procedure is effective in inhibiting the growth of hepatic metastasis of mouse colon carcinoma CT-26 cells.[12] However, we also found that the IFN gene transfer by this procedure was only marginally effective against pulmonary metastasis of the tumor cells. This was associated with the transient concentration of the IFNs in the lung tissue as well as in plasma after the injection of the conventional pDNA encoding IFN-β or IFN-γ.

Systemic administration of a pDNA/cationic liposome complex, or lipoplex, induces several inflammatory cytokines, hematologic changes, and increases the plasma levels of liver enzymes and acute-phase response proteins.[13,14] Such responses can be used as stimuli for transiently increasing pDNA-based transgene expression through the activation of nuclear factor κB.[15] In addition, the nonspecific induction of inflammatory cytokines would be beneficial for cancer gene therapy. However, inflammatory cytokines are reported to reduce the transgene expression at a later time after gene transfer.[16] Early studies have demonstrated that unmethylated CpG dinucleotides in pDNA play significant roles in the induction of inflammatory cytokines through the Toll-like receptor (TLR)-9 upon administration of lipoplex.[17] The cytosine residue of unmethylated CpG dinucleotides in pDNA can also be a target for methylation by DNA methyltransferases.[18,19] Methylated CpG dinucleotides, in turn, recruit the methyl-CpG binding proteins such as MBD1 and MeCP2, which mediate transcriptional repression of the transgene.[20,21] Therefore, the presence of CpG dinucleotides in pDNA may have two adverse consequences: the generation of an inflammatory cytokine response through TLR-9 and the chronic suppression of transgene expression induced by the methylation of CpG dinucleotides as well as by the binding of methyl-CpG binding proteins.

Several approaches have been reported to reduce the number of CpG dinucleotides in pDNA, including the use of polymerase chain reaction (PCR) fragments of pDNA,[22] methylation of the cysteine in CpG dinucleotides by methylase,[23] and the elimination of the sequences.[24] Yew *et al.*[25–27] have reported that a

Abbreviations: AUC, area under the plasma concentration-time curve; C_{max}, peak plasma concentration; FCS, fetal calf serum; HBSS, Hanks' balanced salt solution; IFN, interferon; MRT, mean residence time; PCR, polymerase chain reaction; pDNA, plasmid DNA; TLR, Toll-like receptor.

Grant sponsors: the Ministry of Education, Culture, Sports, Science and Technology, Japan; the Ministry of Health, Labour and Welfare, Japan; the Uehara Memorial Foundation; the Sankyo Foundation of Life Science.

***Correspondence to:** Department of Biopharmaceutics and Drug Metabolism, Graduate School of Pharmaceutical Sciences, Kyoto University, Sakyo-ku, Kyoto 606-8501, Japan. Fax: +81-75-753-4614.
E-mail: takakura@pharm.kyoto-u.ac.jp

Received 25 August 2006; Accepted after revision 9 January 2007
DOI 10.1002/ijc.22636
Published online 19 March 2007 in Wiley InterScience (www.interscience.wiley.com).

UICC Publication of the International Union Against Cancer

CpG-reduced pDNA, pGZB, in which about 80% of the CpG sequences were depleted from the original vector, showed sustained and enhanced transgene expression after administration to mice in several formulations, such as the naked pDNA and lipoplex. Therefore, the use of the CpG-reduced pDNA may improve the efficacy of IFN gene therapy in various tumor models. In the present study, we inserted murine IFN-β or IFN-γ cDNA into the pGZB vector and examined first whether the expression of the IFNs could be improved by the vector. The expression of the IFNs was quantitatively evaluated using a moment analysis method and the parameters obtained, such as the area under the plasma concentration-time curve (AUC) and mean retention time (MRT), were compared with those obtained after injection of a conventional CpG-replete vector. Then, we examined the therapeutic efficacy of pGZB-based IFN gene delivery by the hydrodynamics-based procedure against the lung metastasis produced by CT-26 cells in mice.

Material and methods

Cell cultures and mice

A mouse colon carcinoma cell line, CT-26, was cultured in RPMI1640 supplemented with 10% fetal calf serum (FCS). L cells were cultured in 2 g/l glucose-containing Eagle's minimal essential medium supplemented with 6% FCS. Seven-week-old BALB/c mice, purchased from Shizuoka agricultural cooperative association for laboratory animals (Shizuoka, Japan), were maintained under conventional housing conditions. All animal experiments were conducted in accordance with the principles and procedures outlined in the US National Institutes of health guide for the care and use of laboratory animals. The protocols for animal experiments were approved by the Animal Experimentation Committee of Graduate School of Pharmaceutical Sciences, Kyoto University.

Plasmid DNA

pCMV-Luc, pCMV-Muβ and pCMV-Muγ, which were constructed as previously reported,[28,29] were used as CpG-replete pDNA encoding firefly luciferase, mouse IFN-β and mouse IFN-γ, respectively. pGZB vector,[24–27] a CpG-reduced pDNA that has a backbone different from pCMV vectors, was kindly provided by Dr. Yew (Genzyme Corporation, MA, USA). A fragment of mouse *IFN*-β cDNA was amplified by PCR from pCMV-Muβ, and inserted into the *Sfi*I/*Eco*RI site of the pGZB vector to construct pGZB-Muβ. pGZB-Muγ and pGZB-Luc were also constructed in a similar manner. Each pDNA was injected into the tail vein of mice at the indicated doses dissolved in 1.6 ml saline by the hydrodynamics-based procedure.[3,6] The dose of each pDNA was optimized by preliminary experiments; it was set at 10 μg/mouse for IFN-β-expressing pDNA, which was the same dose as in the previous study.[12] Because the injection of pGZB-Muγ at this high dose was found to be lethal to mice, 3 μg was used for IFN-γ-expressing pDNA.

Measurement of TNF-α concentration

The levels of TNF-α in serum were measured using an ELISA kit (AN'ALYZA™, Genzyme, Cambridge, MA) as reported previously.[15] In brief, mice received an intravenous injection of naked pCMV-Luc or pGZB-Luc at a dose of 25 μg/mouse by the hydrodynamics-based procedure. At 1.5 hr after injection, blood was collected from the vena cava of mice under anesthesia, and allowed to stand for 3 hr at 4°C. Then the samples were centrifuged at 3,000*g* for 30 min at 4°C and the serum obtained was used for the assay.

Measurement of IFN activity

To measure the IFN activity in mouse serum, 50–70 μl blood was collected from the tail vein at indicated times after pDNA injection. The blood samples were kept at 4°C for 2–3 hr to allow clotting and then centrifuged to obtain serum. The antiviral activity of IFN-β in the serum was measured using the cytopathic effect of vesicular stomatitis virus on L cells and expressed in international units (IU) as calibrated against the international reference mouse IFN-α, β preparation (NIH-G002-904-511).[30] The concentration of IFN-γ in the serum was determined by ELISA using a commercial kit (Ready-SET-Go! Mouse IFN-γ ELISA, eBioscience). The peak plasma concentrations (C_{max}) of IFNs were obtained from the actual data recorded after gene transfer. The AUC and MRT were calculated by integration to infinite time.[31] The normal distribution test was performed using the following equation.[32]

$$Z_0 = \frac{\left|\bar{\phi}_1 - \bar{\phi}_2\right|}{\sqrt{SE_1^2 + SE_2^2}}$$

where $\bar{\phi}_1$ and $\bar{\phi}_2$ are the means of pharmacokinetic parameters, and SE_1 and SE_2 are the variances in groups 1 and 2, respectively. If $Z_0 > 1.96$ (confidence interval $p < 0.05$), the difference was assumed to be significant between groups 1 and 2.

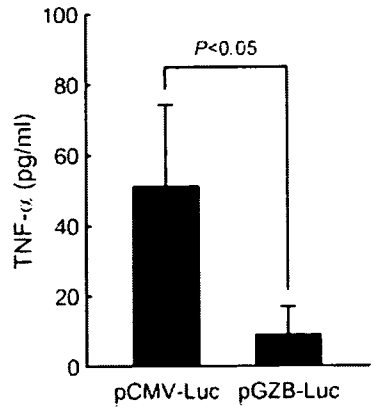

FIGURE 1 – TNF-α level in serum after intravenous injection of pCMV-Luc or pGZB-Luc at a dose of 25 μg/mouse by the hydrodynamics-based procedure. At 1.5 hr after injection, mice were euthanized and blood was collected. Serum concentrations of TNF-α were determined by ELISA. The results are expressed as the mean ± S.D. of 3 mice.

Experimental pulmonary metastasis

CT-26 cells were trypsinized and suspended in Hanks' balanced salt solution (HBSS). The cell suspensions were injected intravenously into syngeneic BALB/c mice at a dose of 1×10^5 cells in 200 μl HBSS/mouse to establish pulmonary metastasis. Mice inoculated with CT-26 cells were injected intravenously with pDNA by the hydrodynamics-based procedure at indicated times. At 14 days after inoculation of the tumor cells, the lung was excised and the number of pulmonary colonies was counted. In addition, the survival of mice was also evaluated in different animals.

Statistical analysis

Data on the number of metastatic colonies were analyzed by one-way ANOVA followed by the Student-Newmann-Keuls multiple comparison test. Survival of mice was analyzed by a Kaplan-Meier survival plot followed by a log-rank (Mantel-Cox) test.

Results

TNF-α production after injection of pCMV-Luc and pGZB-Luc

Figure 1 shows the TNF-α concentration in mouse serum 1.5 hr after intravenous injection of pCMV-Luc or pGZB-Luc at a dose of 25 μg/mouse by the hydrodynamics-based procedure. Previous studies indicated that the TNF-α concentration in serum has a

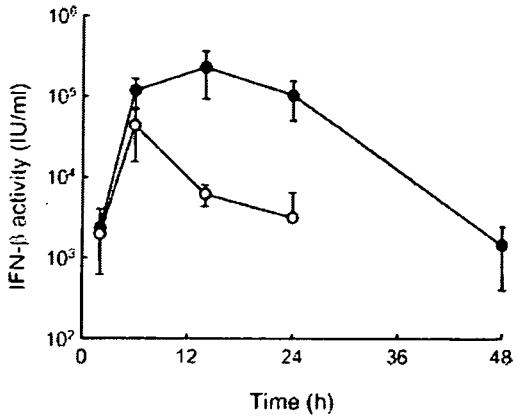

FIGURE 2 – Time-course of the activity of IFN-β in the serum after intravenous injection of pCMV-Muβ (○) or pGZB-Muβ (●) at a dose of 10 μg/mouse by the hydrodynamics-based procedure. The IFN-β activity was measured by bioassay. The activity at 48 hr after injection of pCMV-Muβ was below 400 IU/ml, which is not shown in the figure. The results are expressed as the mean ± SD of 3 mice.

TABLE I – C_{MAX}, AUC AND MRT OF SERUM IFN-β AFTER INTRAVENOUS INJECTION OF PCMV-MUβ AND PGZB-MUβ INTO MICE BY THE HYDRODYNAMICS-BASED PROCEDURE

pDNA	C_{max} (IU/ml)	AUC (IU hr/μl)	MRT (hr)
pCMV-Muβ	43,000 ± 27,800	334 ± 126	8.1 ± 2.6
pGZB-Muβ	227,000 ± 134,000	4,520 ± 650*	16.7 ± 3.6*

The C_{max} values were determined at 6 and 14 h after intravenous injection of pCMV-Muβ and pGZB-Muβ, respectively, by the hydrodynamics-based procedure at a dose of 10 μg/mouse, and are expressed as the mean ± SD of three mice. The AUC and MRT were calculated by integration to infinite time, and are expressed as the calculated mean ± SE.

*Statistically significant ($p < 0.05$) compared with pCMV-Muβ.

peak value around 1.5 hr after injection of various pDNA formulations. The injection of the CpG-replete pCMV-Luc resulted in the peak TNF-α concentration of 51 ± 23 pg/ml, which was significantly greater than that of pGZB-Luc (8.9 ± 8.0 pg/ml). However, these levels of TNF-α production were much lower than those obtained with pDNA/cationic liposome complexes, some of which resulted in a peak TNF-α concentration of 500 pg/ml or greater at the same dose of pDNA.[12,15]

IFN-β activity after injection of pCMV-Muβ and pGZB-Muβ

Figure 2 shows the time-courses of the IFN-β concentrations in serum after intravenous injection of pCMV-Muβ or pGZB-Muβ at a dose of 10 μg/mouse. High IFN-β activities were detected after injection of pCMV-Muβ by the hydrodynamics-based procedure with a peak level of 43,000 ± 27,800 IU/ml at 6 hr after injection. However, the activity declined quickly with time and was below 400 IU/ml by 48 hr. In contrast, the IFN-β activities after injection of pGZB-Muβ were significantly greater than those of pCMV-Muβ at any sampling point except for 2 hr. About a 5-fold greater peak level (227,000 ± 134,000 IU/ml) was obtained at 14 hr after injection, and a significant level of activity could be detected at 48 hr after injection. Table I summarizes the pharmacokinetic parameters of serum IFN-β after injection of each IFN-β-expressing pDNA. The AUC values were calculated to be 334 ± 126 and 4,520 ± 650 IU hr/l after injection of pCMV-Muβ and pGZB-Muβ ($p < 0.05$), respectively, indicating that about a 14-fold greater amount of IFN-β was produced from pGZB-Muβ than from pCMV-Muβ. A long MRT (16.7 ± 3.6 hr) was obtained with pGZB-Muβ, which was statistically ($p < 0.05$) significantly different from that of pCMV-Muβ (8.1 ± 2.6 hr).

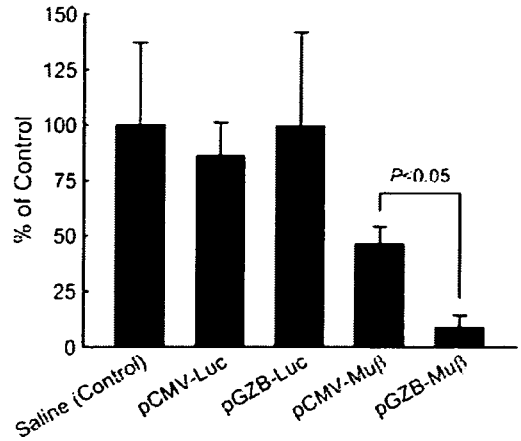

FIGURE 3 – Effect of IFN-β gene transfer on the pulmonary metastasis of CT-26 cells in mice. Mice were inoculated with CT-26 cells by a tail vein injection at a dose of 1×10^5 cells/mouse (day 0). At 24 hr after inoculation, mice were injected intravenously with saline (control), pCMV-Luc, pGZB-Luc, pCMV-Muβ or pGZB-Muβ at a dose of 10 μg/mouse by the hydrodynamics-based procedure. On day 14, mice were euthanized and the number of metastatic colonies on the lung surface was counted. The results are normalized to the control value (226 ± 84, the saline-treated group) and are expressed as the mean ± SD of at least 4 mice.

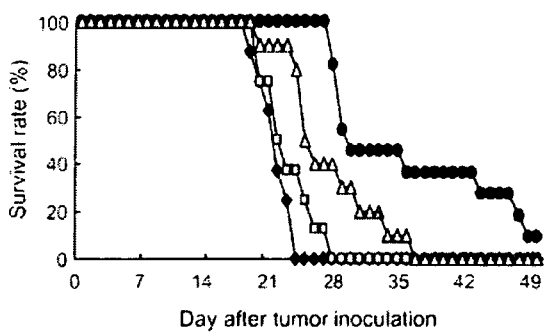

FIGURE 4 – Effect of IFN-β gene transfer on the survival rate of mice bearing pulmonary metastasis of CT-26 cells. Mice inoculated with 1×10^5 CT-26 cells were treated with saline (control, ◆), pCMV-Luc (□), pCMV-Muβ (△) or pGZB-Muβ (●) at a dose of 10 μg/mouse by the hydrodynamics-based procedure at 24 hr after tumor inoculation. Each group consisted of at least 9 mice.

Effects of IFN-β-expressing pDNA on pulmonary metastasis in mice

Inoculation of CT-26 cells into the tail vein of mice resulted in the formation of 226 ± 84 metastatic colonies on the lung surface at 14 days (Fig. 3). pCMV-Muβ or pGZB-Muβ (10 μg/mouse) significantly reduced the number of metastatic colonies following a single injection at 24 hr after the inoculation of CT-26 cells: 46.3% ± 7.9% and 8.6% ± 5.6% of the colonies were found in pCMV-Muβ-treated and pGZB-Muβ-treated mice, respectively, compared with the number in the saline-treated controls. pCMV-Luc (86.0% ± 15.1%) or pGZB-Luc (99.3% ± 42.5%) had little effect on the number of metastatic colonies in mouse lung at the same dose (10 μg), suggesting that the reduction in the number of metastatic colonies is mediated by IFN-β activity.

Figure 4 shows the survival rate of CT-26-bearing mice receiving a single injection of each pDNA (10 μg/mouse). The pCMV-Muβ- or pGZB-Muβ-treated mice survived significantly ($p < 0.05$) longer than the pCMV-Luc-treated mice. The mean survival

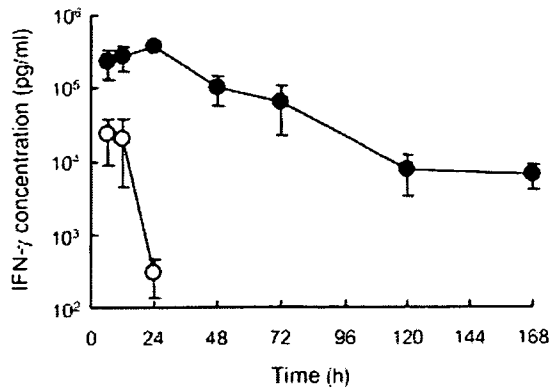

FIGURE 5 – Time-course of the concentration of IFN-γ in serum after intravenous injection of pCMV-Muγ (○) or pGZB-Muγ (●) at a dose of 3 μg/mouse by the hydrodynamics-based procedure. The IFN-γ concentration was measured by ELISA. The concentrations at 36 hr or later after injection of pCMV-Muγ were below the detection limit of 15 pg/ml. The results are expressed as the mean ± SD of at least 3 mice.

TABLE II – C_{MAX}, AUC AND MRT OF SERUM IFN-γ AFTER INTRAVENOUS INJECTION OF PCMV-MUγ AND PGZB-MUγ INTO MICE BY THE HYDRODYNAMICS-BASED PROCEDURE

pDNA	C_{max} (pg/ml)	AUC (pg hr/μl)	MRT (hr)
pCMV-Muγ	23,300 ± 14,700	262 ± 38	8.9 ± 1.8
pGZB-Muγ	382,000 ± 50,600*	15,900 ± 900*	34.8 ± 3.7*

The C_{max} values were obtained at 6 hr and 24 hr after intravenous injection of pCMV-Muβ and pGZB-Muβ, respectively, by the hydrodynamics-based procedure at a dose of 3 μg/mouse, and are expressed as the mean ± SD of at least three mice. The AUC and MRT were calculated by integration to infinite time, and are expressed as the calculated mean ± SE.

*Statistically significant ($p < 0.05$) compared with pCMV-Muγ.

times of mice treated with pCMV-Luc, pCMV-Muβ and pGZB-Muβ were 20.8 ± 1.5, 22.8 ± 3.1 and 26.6 ± 5.1 days, respectively. No statistically significant difference was obtained between the pCMV-Muβ and pGZB-Muβ-treated groups as far as the survival of CT-26-bearing mice was concerned.

IFN-γ concentration after injection of pCMV-Muγ and pGZB-Muγ

Figure 5 shows the time-courses of the IFN-γ concentration in serum after intravenous injection of pCMV-Muγ or pGZB-Muγ at a dose of 3 μg/mouse. Again, sustained IFN-γ concentrations were observed in mice receiving CpG-reduced pGZB-Muγ. More than 10,000 pg IFN-γ/ml was detected in the serum from 6 hr to 3 days after injection of pGZB-Muγ, whereas the concentrations were below the detection limit at 36 hr or later after injection of pCMV-Muγ. The initial IFN-γ concentration after injection of pGZB-Muγ was much greater than that after pCMV-Muγ ($p < 0.05$). In addition, the IFN concentration declined with a longer half-life in mice receiving pGZB-Muγ than in those receiving pCMV-Muγ, suggesting prolonged expression of IFN-γ by pGZB-Muγ. These expression properties of both vectors resulted in significant differences ($p < 0.05$) in the pharmacokinetic parameters (Table II): more than a 60-fold greater AUC and an about 4-fold longer MRT were obtained when pGZB-Muγ was injected in place of pCMV-Muγ.

Effects of IFN-γ-expressing pDNA on pulmonary metastasis in mice

Mice receiving CT-26 cells by intravenous injection were injected intravenously with pGZB-Muγ, pCMV-Muγ, pGZB-Luc or pCMV-Luc (3 μg/mouse) by the hydrodynamics-based procedure at 1 day after tumor inoculation. Figure 6 shows the number of metastatic colonies on the lung surface measured at 14 days

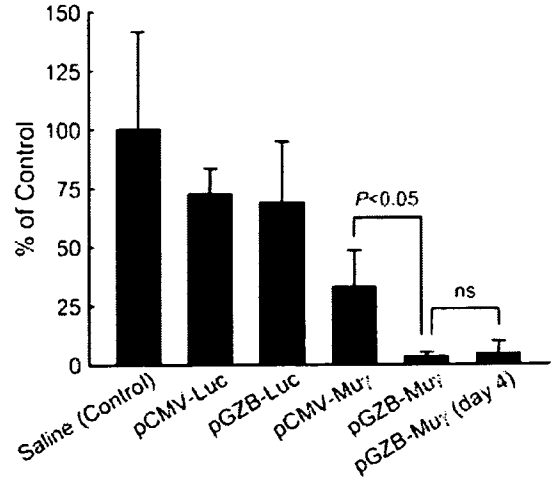

FIGURE 6 – Effect of IFN-γ gene transfer on the pulmonary metastasis of CT-26 cells in mice. Mice were inoculated with CT-26 cells by a tail vein injection at a dose of 1×10^5 cells/mouse (day 0). At 24 hr after inoculation, mice were injected intravenously with saline (control), pCMV-Luc, pGZB-Luc, pCMV-Muγ or pGZB-Muγ at a dose of 3 μg/mouse by the hydrodynamics-based procedure. On day 14, mice were euthanized and the number of metastatic colonies on the lung surface was counted. The results are normalized to the control value (215 ± 89, the saline-treated group) and are expressed as the mean ± SD of at least 4 mice.

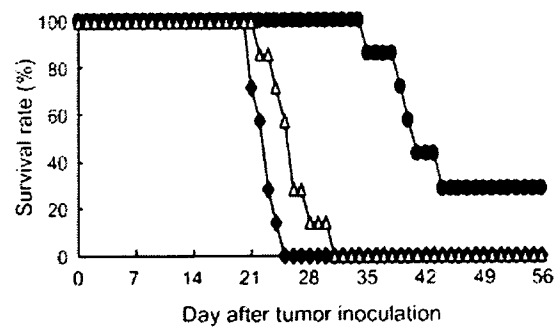

FIGURE 7 – Effect of IFN-γ gene transfer on the survival rate of mice bearing pulmonary metastasis of CT-26 cells. Mice inoculated with 1×10^5 CT-26 cells were treated with saline (control, ◆), pCMV-Muγ (△) or pGZB-Muγ (●) at a dose of 3 μg/mouse by the hydrodynamics-based procedure at day 1, 14, and 28 after tumor inoculation. Each group consisted of at least 7 mice.

after inoculation. pCMV-Muγ and pGZB-Muγ reduced the number of colonies to 32.8% ± 15.7% and 3.4% ± 1.7% of those in the saline-treated group (215 ± 89 colonies). To examine the effect of the interval of tumor inoculation and IFN-γ gene transfer, pGZB-Muγ was injected 4 days after tumor inoculation. This treatment also reduced the number of colonies to 4.4% ± 5.5% of those in the saline-treated group, which was not significantly different from the pGZB-Muγ-treated group injected 1 day after tumor inoculation. No significant reduction was obtained by pCMV-Luc (72.7% ± 10.7%) or pGZB-Luc (69.1% ± 25.9 %). Then, the survival of CT-26-bearing mice was examined in different sets of mice, which received 3 injections of pCMV-Muγ or pGZB-Muγ (3 μg/mouse/shot) at day 1, 14 and 28 after tumor inoculation (Fig. 7). The mean survival times of the saline-treated group and the pCMV-Muγ-treated group were 21.7 ± 1.5 and 25.0 ± 2.9 days, respectively, and the difference was not statistically significant. In contrast, the survival time of the pGZB-Muγ-treated mice